

Affine-Invariant Integrated Rank-Weighted Depth: Definition, Properties and Finite Sample Analysis

Guillaume Staerman¹ Pavlo Mozharovskiy¹ Stéphan Cléménçon¹

Abstract

Because it determines a center-outward ordering of observations in \mathbb{R}^d with $d \geq 2$, the concept of statistical depth permits to define quantiles and ranks for multivariate data and use them for various statistical tasks (e.g. inference, hypothesis testing). Whereas many depth functions have been proposed *ad-hoc* in the literature since the seminal contribution of Tukey (1975), not all of them possess the properties desirable to emulate the notion of quantile function for univariate probability distributions. In this paper, we propose an extension of the *integrated rank-weighted* statistical depth (IRW depth in abbreviated form) originally introduced in Ramsay et al. (2019), modified in order to satisfy the property of *affine-invariance*, fulfilling thus all the four key axioms listed in the nomenclature elaborated by Zuo & Serfling (2000). The variant we propose, referred to as the Affine-Invariant IRW depth (AI-IRW in short), involves the precision matrix of the (supposedly square integrable) d -dimensional random vector X under study, in order to take into account the directions along which X is most variable to assign a depth value to any point $x \in \mathbb{R}^d$. The accuracy of the sampling version of the AI-IRW depth is investigated from a non-asymptotic perspective. Namely, a concentration result for the statistical counterpart of the AI-IRW depth is proved. Beyond the theoretical analysis carried out, applications to anomaly detection are considered and numerical results are displayed, providing strong empirical evidence of the relevance of the depth function we propose here.

1. Introduction

Since its introduction in Tukey (1975), the concept of statistical depth has become increasingly popular in multivariate data analysis. For a distribution P on \mathbb{R}^d with $d > 1$, by transporting the natural order on the real line to \mathbb{R}^d , a depth function $D(\cdot, P) : \mathbb{R}^d \rightarrow \mathbb{R}_+$ provides a center-outward ordering of points in the support of P and can be straightforwardly used to extend the notions of (signed) rank or order statistics to multivariate data, which find numerous applications in Statistics and Machine Learning (e.g. robust inference, hypothesis testing, novelty/anomaly detection), see Mosler (2013) for instance. Numerous definitions have been proposed, as alternatives to the earliest proposal, the *halfspace* depth introduced in Tukey (1975): among many others, the simplicial depth (see Liu (1990)), the projection depth (Liu (1992)), the majority depth (Liu & Singh (1993)), the Oja depth (Oja (1983)), the zonoid depth (Koshevoy & Mosler (1997)), the spatial depth (Chaudhuri (1996) or Vardi & Zhang (2000)) or the Monge-Kantorovich depth (see Chernozhukov et al. (2017)). In order to compare systematically their merits and drawbacks, Zuo & Serfling (2000) have devised an axiomatic nomenclature of statistical depths, listing key properties that should be ideally satisfied by a depth function. Roughly, as depth functions serve to define center-outward orderings, if a distribution P on \mathbb{R}^d has a unique center $\theta \in \mathbb{R}^d$ (i.e. a symmetry center in a certain sense), the latter should be the deepest point and the depth should decrease along any fixed ray through it. One also expects that a depth function vanishes at infinity and does not depend on the coordinate system chosen. This latter property is usually formulated as *affine-invariance*. A more formal description of these four properties is given in Section 2. Beyond the verification of these properties, the pros and cons of any data depth should be considered with regard to the possible existence of algorithms for exact computation in the case of discrete/sampling distributions. In this respect, the extension of Tukey's halfspace depth recently introduced in Ramsay et al. (2019) and referred to as the integrated rank-weighted (IRW) depth offers many advantages. Rather than computing, for any point x in \mathbb{R}^d , the minimum of the mass $P(\mathcal{H})$ taken over all closed half-spaces $\mathcal{H} = \{x' \in \mathbb{R}^d : \langle x' - x, u_{\mathcal{H}} \rangle \leq 0\}$ with unit normal vector $u_{\mathcal{H}} \in \mathbb{R}^d$ and containing x , it is proposed to

¹LTCI, Télécom Paris, Institut Polytechnique de Paris. Correspondence to: Guillaume Staerman <guillaume.staerman@telecom-paris.fr>.

replace the infimum by the integral taken w.r.t. all possible directions $u_{\mathcal{H}}$ uniformly (w.r.t. the uniform distribution on the unit sphere), following in the footsteps of the general *integrated dual depth* approach developed in Cuevas & Fraiman (2009). For a discrete/empirical distribution, the depth thus constructed admits a weighted average representation and can be easily approximated by means of Monte-Carlo methods in contrast to many other depth functions, whose values are defined as solutions of optimization problems, possibly very complex in high dimension. Beyond these computational aspects, it is shown in Ramsay et al. (2019) that the IRW data depth satisfies several desirable properties, see Theorem 2 therein. Unfortunately, it does not fulfill the *affine-invariance* property, as the values taken by the IRW depth may possibly highly depend on the coordinate system chosen to represent the statistical information available, as shown by an illustrative example in the Appendix section. It is the main purpose of this paper to overcome the lack of affine invariance of the IRW depth by proposing a modified version of it, named AI-IRW. It consists in the IRW depth of the (supposedly square integrable) random vector X with distribution P under study expressed in an orthogonal coordinate system such that its components are linearly uncorrelated, i.e. of the random vector whose components are the principal components of X obtained by eigenvalue decomposition of its covariance matrix Σ (Principal Component Analysis). Under the assumption that Σ is definite positive (otherwise, the methodology promoted should be naturally applied after a dimensionality reduction step, i.e. applied to an appropriate orthogonal projection of the original random vector X), the *affine-invariant* version of the IRW depth (the AI-IRW depth in abbreviated form) of X is the IRW depth of $\Sigma^{-1/2}X$, denoting by $\Sigma^{-1/2}$ the inverse of the matrix $\Sigma^{1/2}$, the square root of the symmetric positive definite matrix Σ . In this article, we show that the AI-IRW depth inherits all the properties and computational advantages of the IRW depth and satisfies the *affine-invariance* property in addition. Because its statistical counterpart based on a sample composed of independent copies of the random variable X is a complex functional of the data, involving the square root of the empirical precision matrix, a finite-sample analysis is carried out here. Precisely, a concentration result for the sampling version of the AI-IRW depth is established. Beyond this theoretical analysis, the relevance of the AI-IRW depth notion is also supported by experimental results, showing its advantages over the IRW depth and other depth proposals standing as natural competitors when applied to various statistical tasks such as anomaly detection.

The article is structured as follows. In Section 2, the concept of data depth is briefly reviewed, together with illustrating examples, the integrated rank-weighted depth in particular, and the axiomatic approach developed by Zuo & Serfling (2000).

In Section 3, the AI-IRW depth is introduced, its properties are studied and approximation/estimation issues are discussed at length. The accuracy of the empirical version is investigated in Section 4 from a nonasymptotic perspective. Section 5 describes experimental results illustrating empirically the advantages of the AI-IRW depth. Finally, some concluding remarks are collected in Section 6. Additional technical details and numerical results are deferred to the Appendix section.

2. Background and Motivations

The concept of depth function is motivated by the desire to extend the very useful notions of order and (signed) rank statistics in univariate statistical analysis to multivariate situations by means of depth-induced contours. Indeed, such statistics serve to perform a wide variety of tasks, ranging from robust statistical inference to efficient statistical hypothesis testing for instance. The earliest proposal is the halfspace depth developed in Tukey (1975), whose popularity arises in particular from its strong connection with the notion of distribution function in the univariate context. Indeed, for any probability measure P_1 on \mathbb{R} , constructed as a median-oriented distribution function, the univariate halfspace depth is given by: $\forall t \in \mathbb{R}$,

$$D_{H,1}(t, P_1) = \min \{P_1([-\infty, t]), P_1((t, +\infty])\}.$$

Considering a multivariate r.v. X with probability distribution P on \mathbb{R}^d with $d > 1$, its halfspace depth at $x \in \mathbb{R}^d$ is then defined as the infimum of the probability mass taken over all possible closed halfspaces containing x :

$$D_H(x, P) = \inf_{u \in \mathbb{S}^{d-1}} \mathbb{P}(\langle u, X \rangle \leq \langle u, x \rangle), \quad (1)$$

denoting by $\langle \cdot, \cdot \rangle$ and $\|\cdot\|$ the usual Euclidean inner product and norm on \mathbb{R}^d , by $\mathbb{S}^{d-1} = \{z \in \mathbb{R}^d : \|z\| = 1\}$ the unit sphere of \mathbb{R}^d w.r.t. the Euclidean norm. The halfspace depth (1), probably because of some of its appealing properties (it is quasi-concave, upper semi-continuous), is undeniably the most documented notion of depth function in the statistical literature. It has been proved to fully characterize discrete/empirical distributions in Struyf & Rousseeuw (1999); Koshevoy (2002). Asymptotic guarantees (consistency, asymptotic normality) for its sampling version based on independent copies X_1, \dots, X_n of the generic r.v. X (obtained by replacing P in (1) with the empirical distribution $\hat{P} = (1/n) \sum_{i=1}^n \delta_{X_i}$, where δ_x means the Dirac mass at any point x) are established in e.g. Rousseeuw & Struyf (1998); Donoho (1982); Zuo & Serfling (2000). Multivariate location estimators based on it have been investigated in Donoho & Gasko (1992) and it has been shown to possess attractive robustness properties. For instance, the asymptotic breakdown point of the Tukey median, i.e. the barycenter of the deepest locations in the sense of (1), is equal to $1/3$ for

absolutely continuous centrosymmetric distributions, see [Donoho & Gasko \(1992\)](#). Computational issues have also been extensively studied, see [Liu & Zuo \(2014\)](#) or [Liu et al. \(2018\)](#) for instance. However, as recalled in the Introduction section, many other notions of depth have been proposed these last decades, far too numerous to be listed in an exhaustive manner here, refer to [Mosler \(2013\)](#) for an excellent account of the statistical depth theory. In order to guarantee the “center-outward ordering” interpretation of a depth function $D(\cdot, P) : \mathbb{R}^d \rightarrow \mathbb{R}_+$ of a probability distribution P on \mathbb{R}^d , four key properties have been listed by [Zuo & Serfling \(2000\)](#), see also [Dyckerhoff \(2004\)](#) and [Mosler \(2013\)](#) for a different formulation of the latter. They are recalled below.

D₁ (AFFINE INVARIANCE) Denoting by P_X the distribution of any r.v. X taking its values in \mathbb{R}^d , we have

$$\forall x \in \mathbb{R}^d, \quad D(Ax + b, P_{AX+b}) = D(x, P_X),$$

for any d -dimensional r.v. X , any $d \times d$ nonsingular matrix A with real entries and any vector b in \mathbb{R}^d .

D₂ (MAXIMALITY AT CENTER) For any probability distribution P on \mathbb{R}^d that possesses a symmetry center x_P (in a sense to be specified), the depth function $D(\cdot, P)$ takes its maximum value at it:

$$D(x_P, P) = \sup_{x \in \mathbb{R}^d} D(x, P).$$

D₃ (MONOTONICITY RELATIVE TO DEEPEST POINT) For any probability distribution P on \mathbb{R}^d with deepest point x_P , the depth at any point x in \mathbb{R}^d decreases as one moves away from x_P along any ray passing through it:

$$\forall \alpha \in [0, 1], \quad D(x_P, P) \geq D(x_P + \alpha(x - x_P), P).$$

D₄ (VANISHING AT INFINITY) For any probability distribution P on \mathbb{R}^d , the depth function D vanishes at infinity:

$$D(x, P) \rightarrow 0, \text{ as } \|x\| \rightarrow \infty.$$

It is worth mentioning that the most general notion of symmetry when analyzing data depth is the halfspace symmetry and will be the one we rely on in the paper. Precisely, the probability distribution P is halfspace symmetric in x_P if $P(\mathcal{H}_{x_P}) \geq 1/2$ for all closed halfspaces \mathcal{H}_{x_P} passing through x_P .

Various works have examined which of the properties, among those listed above, are satisfied by specific notions of depth introduced in the literature, see [Zuo & Serfling \(2000\)](#). Some of them are constructed as an infimum over unit-sphere projections of a univariate non parametric statistic such as the projection depth proposed by [Liu \(1992\)](#) or

those introduced in [Zhang \(2002\)](#) or [Zuo \(2003\)](#). From a practical perspective, computing these projection-based depths involves the use of tools such as manifold optimization algorithms, facing various numerical difficulties as the dimension d increases, see [Dyckerhoff et al. \(2021\)](#). In addition, the halfspace depth suffers from two major problems: (i) for each data point, taking the direction achieving the minimum to assign a score to it possibly creates a significant sensitivity to noisy directions (ii) the null score assigned to each new data point outside of the convex hull of the support of the distribution P makes the score of such points indistinguishable. A remedy based on Extreme Value Theory has been proposed in [Einmahl et al. \(2015\)](#), which consists in smoothing the halfspace depth beyond the convex hull of the data. However, this variant relies on rather rigid parametric assumptions, is only approximately affine invariant and confronted with the limitation aforementioned regarding the non-smoothed part of the data. Recently, alternative depth functions have been proposed, obtained by replacing the infimum over all possible directions by an integral, see [Cuevas & Fraiman \(2009\)](#). In [Ramsay et al. \(2019\)](#), a new data depth, referred to as the Integral Rank-Weighted (IRW) depth, is defined by substituting an integral over the sphere \mathbb{S}^{d-1} for the infimum in (1). Here and throughout, the indicator function of any event \mathcal{E} is denoted by $\mathbb{I}\{\mathcal{E}\}$, the spherical probability measure on \mathbb{S}^{d-1} by ω_{d-1} .

Definition 2.1 ([Ramsay et al. \(2019\)](#)). *The Integrated Rank-Weighted (IRW) depth of $x \in \mathbb{R}^d$ relative to a probability distribution P on \mathbb{R}^d is given by:*

$$D_{IRW}(x, P) = \int_{\mathbb{S}^{d-1}} D_{H,1}(\langle u, x \rangle, P_u) \omega_{d-1}(du) \quad (2)$$

$$= \mathbb{E}[D_{H,1}(\langle U, x \rangle, P_U)],$$

where P_u is the pushforward distribution of P defined by the projection $x \in \mathbb{R}^d \mapsto \langle u, x \rangle$ and U is a r.v. uniformly distributed on the hypersphere \mathbb{S}^{d-1} .

As explained at length in [Ramsay et al. \(2019\)](#), the name of the data depth (2) originates from the fact that it can be represented as a weighted average of a finite set of normalized center-outward ranks. It has many advantages over the original halfspace depth (1). First, by construction it is *robust* to noisy directions and *sensitive* to new data point outside of the convex hull of the training data set both at the same time, fixing then the two problems mentioned above. Moreover, concerning numerical feasibility, the computation of the IRW depth does not require to implement any manifold optimization algorithm and can be approximately made by means of basic Monte Carlo techniques, providing in addition confidence intervals as a by-product, see Remark 2.2 below. Its contours $\{D_{IRW}(x, P) = \alpha\}$, $\alpha \in [0, 1]$, also exhibits a higher degree of smoothness in general (the depth function (2) is continuous at any point $x \in \mathbb{R}^d$ that is not an atom for P , cf. Proposition 1 in [Ramsay et al. \(2019\)](#)) and

properties \mathbf{D}_2 , \mathbf{D}_3 and \mathbf{D}_4 have been proved to be satisfied by (2) under mild assumptions, see Theorem 2 in Ramsay et al. (2019).

Remark 2.2. (MONTE CARLO APPROXIMATION) Recall that a r.v. uniformly distributed on the hypersphere \mathbb{S}^{d-1} can be generated from a d -dimensional centered Gaussian random vector W with the identity \mathcal{I}_d as covariance matrix: if $W \sim \mathcal{N}(0, \mathcal{I}_d)$, then $W/\|W\| \sim \omega_{d-1}$, see Krantz & Parks (2008). Hence, a basic Monte-Carlo method to approximate (2) would consist in generating $m \geq 1$ independent realizations W_1, \dots, W_m of $\mathcal{N}(0, \mathcal{I}_d)$ and compute

$$\frac{1}{m} \sum_{j=1}^m D_{H,1}(\langle W_j/\|W_j\|, x \rangle, P_{W_j/\|W_j\|}), \quad (3)$$

refer to e.g. Kalos & Whitlock (2008) for an account of Monte Carlo integration methods.

However, it does not satisfy the key property \mathbf{D}_1 (affine-invariance) in general as illustrated in the next section (see also Section A.3 and Section D.1 of the Appendix for an analytical example and for an additional numerical illustration, respectively). The fact that it is affected by non-uniform scaling is problematic in practice (regarding its interpretability in particular or its use for anomaly detection tasks for instance, see Section 5) and is the main flaw of this approach, as pointed out in Cuevas & Fraiman (2009); Ramsay et al. (2019).

3. Affine-Invariant IRW Depth - Definition and Properties

Here we propose to modify the depth function (2) in order to ensure that property \mathbf{D}_1 is always satisfied when the random vector X with distribution P under study is assumed to be square integrable with positive definite covariance matrix Σ . Precisely, rather than taking the expectation w.r.t. a random direction U uniformly distributed on \mathbb{S}^{d-1} (i.e. integrating over all possible directions $u \in \mathbb{S}^{d-1}$), one considers the random projections defined by the eigenfunctions of the matrix Σ , i.e. the principal components of the r.v. X . In other words, the expectation is taken w.r.t. the distribution of the random vector $V = \Sigma^{-\top/2}U/\|\Sigma^{-\top/2}U\|$ valued in \mathbb{S}^{d-1} , yielding the definition below.

Definition 3.1 (AFFINE-INVARIANT IRW DEPTH). The Affine-Invariant Integrated Rank-Weighted (AI-IRW) depth relative to a square integrable random vector X with probability distribution P on \mathbb{R}^d and positive definite covariance matrix Σ is given by:

$$\forall x \in \mathbb{R}^d, \quad D_{AI-IRW}(x, P) = \mathbb{E}[D_{H,1}(\langle V, x \rangle, P_V)], \quad (4)$$

where $V = \Sigma^{-\top/2}U/\|\Sigma^{-\top/2}U\|$ and U is uniformly distributed on the hypersphere \mathbb{S}^{d-1} .

tributed on the hypersphere \mathbb{S}^{d-1} .

Of course, in the case where the covariance matrix Σ of the supposedly square integrable r.v. X is not invertible, the AI-IRW depth notion should be applied to an orthogonal projection, after an appropriate dimensionality reduction step. From a computational perspective, The AI-IRW depth can be approximated by Monte Carlo methods in the same way as (2), see Remark 2.2. As revealed by the proposition stated below, the depth function (4) inherits all the properties of (2) under similar assumptions and is remarkably invariant under any affine transformation in addition.

Proposition 3.2. The assertions below hold true for any probability distribution P of a square integrable r.v. X valued in \mathbb{R}^d with positive definite covariance matrix.

- (i) The AI-IRW depth satisfies the properties \mathbf{D}_1 and \mathbf{D}_4 . In addition, \mathbf{D}_2 and \mathbf{D}_3 hold for halfspace symmetric distributions.
- (ii) The AI-IRW depth function is continuous at each point x that is not an atom for P .

The proof is detailed in Section B.1 of the Appendix. It is known that for elliptical distributions, affine invariant data depth level sets are concentric ellipsoids with the same center and orientation as the density level sets (Liu & Singh, 1993). Therefore, the ordering returned by affine-invariant data depths should be equal to that of the density function. Thus, in order to highlight the discrepancy between AI-IRW and IRW w.r.t. affine-invariance, we propose to compare the ordering returned by AI-IRW and IRW to that of the density function on the Gaussian distribution which belongs to the family of elliptical distributions. As illustrated by the Rank-Rank plots in Figure 1, the ordering defined by the (empirical) AI-IRW depth is generally much closer to that induced by the underlying density than the order defined by the original (IRW depth) version.

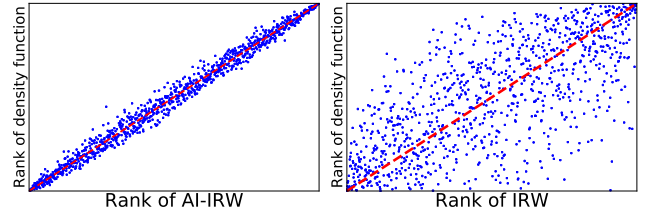


Figure 1. Rank-Rank plots comparing the ranks of 1000 points sampled from a 10-d (anisotropic) Gaussian distribution with covariance matrix drawn at random from a Wishart distribution (with parameters (d, \mathcal{I}_d)) induced by the empirical depth (AI-IRW on the left, IRW on the right) and those induced by the Gaussian density.

In practice, the distribution P is generally unknown as well as the covariance matrix Σ and only a sample $\mathcal{D}_n =$

$\{X_1, \dots, X_n\}$ composed of $n \geq 1$ independent realizations of the distribution P is available. A statistical counterpart of the AI-IRW depth can be obtained by replacing P with the empirical measure $\hat{P} = (1/n) \sum_{i=1}^n \delta_{X_i}$ and $\Sigma^{-\top/2}$ with an estimator $\hat{\Sigma}^{-\top/2}$ based on \mathcal{D}_n and plugging them next into formula (4) when $\hat{\Sigma}$ is invertible, yielding: $\forall x \in \mathbb{R}^d$,

$$\hat{D}_{\text{AI-IRW}}(x) = \mathbb{E} \left[D_{H,1}(\langle \hat{V}, x \rangle, \hat{P}_{\hat{V}}) \mid \mathcal{D}_n \right], \quad (5)$$

where $\hat{V} = \hat{\Sigma}^{-\top/2} U / \|\hat{\Sigma}^{-\top/2} U\|$ and U is a r.v. uniformly distributed on \mathbb{S}^{d-1} independent from the X_i 's. From a practical perspective, the (conditional) expectation (5) can also be approximated by means of a basic Monte Carlo scheme, generating $m \geq 1$ i.i.d. random directions U_1, \dots, U_m , copies of the generic r.v. U and independent from the original data \mathcal{D}_n : $\forall x \in \mathbb{R}^d$,

$$\tilde{D}_{\text{AI-IRW}}^{\text{MC}}(x) = \frac{1}{m} \sum_{j=1}^m \min \left\{ \hat{F}_{\hat{V}_j}(\langle \hat{V}_j, x \rangle), 1 - \hat{F}_{\hat{V}_j}(\langle \hat{V}_j, x \rangle) \right\}, \quad (6)$$

where, for all $j \in \{1, \dots, m\}$ and $t \in \mathbb{R}$, we set

$$\hat{V}_j = \hat{\Sigma}^{-\top/2} U_j / \|\hat{\Sigma}^{-\top/2} U_j\|,$$

and

$$\hat{F}_{\hat{V}_j}(t) = \frac{1}{n} \sum_{i=1}^n \mathbb{I}_{\{\langle \hat{V}_j, X_i \rangle \leq t\}},$$

where $\mathbb{I}_{\mathcal{E}}$ means the indicator function of any event \mathcal{E} . Putting aside the issue of estimating $\Sigma^{-\top/2}$ (discussed below), attention should be paid to the fact that the approximate sample version (6) is very easy to compute (refer to Section C in the Appendix for further details) and involves no optimization procedure, in contrast to many other notions of depth function.

On estimating the square root of the precision matrix.

Consider the $d \times n$ matrix $\mathbf{X}_n = (X_1, \dots, X_n)$ with the X_i 's as columns. The simplest way of building an estimate $\hat{\Sigma}^{-\top/2}$ consists in computing the empirical version of the covariance matrix $\hat{\Sigma} = (1/n) \mathbf{X}_n \mathbf{X}_n^\top$, which is a natural and nearly unbiased estimator, and inverting next its square root, when the latter is positive definite (which happens with overwhelming probability). For simplicity, this is the estimation we consider in the finite-sample study presented in the next section. However, alternative techniques can be used, yielding possibly more efficient estimators under specific assumptions, in high-dimension especially. Shrinkage procedures for covariance estimation under sparsity conditions have been investigated in e.g. Ledoit & Wolf (2004);

Chen et al. (2010); Schäfer & Strimmer (2005), while a lasso method for direct estimation of the precision matrix, avoiding matrix inversion, is proposed in Friedman et al. (2008). Robust covariance estimation techniques, tailored to situations where the data are possibly contaminated or heavy-tailed, have also been documented in the literature, see e.g. Rousseeuw (1984) and Rousseeuw & van Driessen (1999). Classically, from a symmetric definite positive estimator of the covariance matrix, one can easily build an estimator of the square root of the precision matrix by inverting a triangular/diagonal matrix. Due to the presence of $\hat{\Sigma}^{-\top/2}$ in (5) (respectively, in (6)), it is far from straightforward to assess the accuracy of the estimators of the AI-IRW depth proposed above. It is the purpose of the next section to study the uniform deviations between (4) and its empirical versions from a nonasymptotic perspective.

4. Finite-Sample Analysis - Concentration Bounds

We now investigate the accuracy of the statistical version, as well as that of its Monte Carlo approximation, of the AI-IRW depth function introduced in the previous section in a nonasymptotic fashion. Precisely, we establish a concentration bound for the maximal deviations between the true and estimated AI-IRW depth functions. We assume here that the estimator of the square root of the precision matrix is given by the inverse of the square root of the empirical covariance, when the latter is definite positive (which happens with overwhelming probability), and by that of any definite positive regularized version (e.g. Tikhonov) of the latter otherwise. The subsequent analysis requires additional hypotheses, listed below. The first assumption, classical when estimating the precision matrix (see e.g. Cai & Zhou (2013) or Fan et al. (2016)), stipulates that the eigenvalues $\sigma_1, \dots, \sigma_d$ of the covariance matrix Σ of the square integrable random vector X considered are bounded away from zero.

Assumption 4.1. *There exists $\varepsilon > 0$ such that: $\forall k \in \{1, \dots, d\}, \varepsilon \leq \sigma_k$.*

The second assumption is technical, see Davis & Kahan (1970). It stipulates that Σ 's eigenvalues are all of multiplicity 1 and that Σ 's minimum eigengap is bounded away from zero.

Assumption 4.2. *There exists $\gamma > 0$ such that: $\forall k \in \{1, \dots, d-1\}, \gamma \leq \sigma_{(k)} - \sigma_{(k+1)}$, where $\sigma_{(1)} > \dots > \sigma_{(d)}$ are Σ 's eigenvalues sorted by decreasing order of magnitude.*

We point out that, just like when Σ is not invertible, one always may bring back the analysis to a situation where Assumption 4.2 is fulfilled by means of a preliminary dimensionality reduction step. Notice incidentally that, when

$\Sigma = \sigma \mathcal{I}_d$, with $\sigma > 0$, the AI-IRW reduces to IRW. The other assumptions correspond to smoothness conditions of Lipschitz type for the function $\phi : (u, x) \in \mathbb{S}^{d-1} \times \mathbb{R}^d \mapsto \mathbb{P}\{\langle u, X \rangle \leq \langle u, x \rangle\}$.

Assumption 4.3. (UNIFORM LIPSCHITZ CONDITION IN PROJECTION) *For all $(x, y) \in \mathbb{R}^d \times \mathbb{R}^d$, there exists $L_p < +\infty$ such that*

$$\sup_{u \in \mathbb{S}^{d-1}} |\phi(u, x) - \phi(u, y)| \leq L_p \|x - y\|.$$

Assumption 4.4. (UNIFORM RADIAL LIPSCHITZ CONDITION) *For all $(u, v) \in \mathbb{S}^{d-1} \times \mathbb{S}^{d-1}$, there exists $L_R < +\infty$ such that*

$$\sup_{x \in \mathbb{R}^d} |\phi(u, x) - \phi(v, x)| \leq L_R \|u - v\|.$$

Notice that the same assumptions are involved in the non-asymptotic rate bound analysis carried out for the halfspace depth estimator in [Burr & Fabrizio \(2017\)](#) and are used to establish limit results related to its approximation in [Nagy et al. \(2020\)](#). The Lipschitz conditions are satisfied by a large class of probability distributions, for which Lipschitz constants L_R and L_p can be both explicitly derived. For instance, if the distribution P of X has compact support included in the ball $\mathcal{B}(0, r) = \{x \in \mathbb{R}^d : \|x\| \leq r\}$ (relative to the Euclidean norm $\|\cdot\|$) with $r > 0$ and is absolutely continuous w.r.t. the Lebesgue measure with a density bounded by $M > 0$, the uniform Lipschitz conditions are then fulfilled with $L_R = MV_{d,r}$ and $L_p = MV_{d-1,r}$, where $V_{d,r} = \pi^{d/2} r^d / \Gamma(d/2 + 1)$ is the volume of the ball $\mathcal{B}(0, r)$ and $z \geq 0 \mapsto \Gamma(z) = \int_0^\infty t^{z-1} e^{-t} dt$ means the Gamma function, refer to the Appendix section for further details (see Lemma B.1 and B.2 therein) and to [Burr & Fabrizio \(2017\)](#) for additional examples. In contrast, a necessary condition for Assumption 4.3 to be satisfied is the absolute continuity of the measure P w.r.t. the Lebesgue measure, see Section 4 in [Nagy et al. \(2020\)](#). The bounds stated in the theorem below reveal the accuracy of the statistical estimates (5) and (6) and highlight their behavior through explicit constants.

Theorem 4.5. *Suppose that the distribution P of the r.v. X is τ sub-Gaussian and satisfies Assumptions 4.1, 4.2, 4.3 and 4.4. The following assertions hold true.*

- (i) *For any $\delta \in \left(\max\{\Theta, 12.9^d\} e^{-\frac{\tau}{2} \min\{\alpha, \alpha^2, \alpha\Delta/8\}}, 1\right)$, we have with probability at least $1 - \delta$:*

$$\begin{aligned} & \sup_{x \in \mathbb{R}^d} \left| \widehat{D}_{AI-IRW}(x) - D_{AI-IRW}(x, P) \right| \\ & \leq \Delta(L_R, d, \gamma, \varepsilon, \tau) \max_{s=1,2} \left(\frac{d + \log(2/\delta)}{n} \right)^{1/s} \\ & \quad + \sqrt{\frac{8 \log(\Theta/\delta)}{n}}, \end{aligned}$$

where $\Delta = 512L_R\tau^2 \max\{1/\xi, 2\sqrt{2d}/\gamma\}$ with $\xi \in (0, \varepsilon)$, $\alpha(\varepsilon, \tau) = (\varepsilon - \xi)/(32\tau^2)$ and $\Theta = 12(2n)^{d+1}/(d+1)!$.

- (ii) *Let $r > 0$. For any $\delta \in \left(\max\{\Theta, 12.9^d\} e^{-n \min\{\alpha, \alpha^2, \alpha\Delta/8\}}, 1\right)$, we have with probability at least $1 - \delta$:*

$$\begin{aligned} & \sup_{x \in \mathcal{B}_r} \left| \widehat{D}_{AI-IRW}^{MC}(x) - D_{AI-IRW}(x, P) \right| \\ & \leq \sqrt{\frac{128 \log(3\Theta/2\delta)}{9n}} + 2\sqrt{\frac{d \log(3rm) + \log(6/\delta)}{18m}} \\ & \quad + \frac{4L_p}{3m} + \frac{8\Delta}{3} \max_{s=1,2} \left(\frac{d + \log(2/\delta)}{n} \right)^{1/s}, \end{aligned}$$

where the constants Θ , Δ , α and the parameter $\xi \in (0, \varepsilon)$ are the same as those involved in (i).

Due to space limitations, the detailed proof is postponed to the Section B.2 of the Appendix. The upper confidence bound in assertion (i) is decomposed into two terms. The first term, of order $O(n^{-1/2})$, owes its presence to the replacement of $\Sigma^{-1/2}$ by its estimator. The second term, of order $O(\sqrt{\log(n)/n})$ and exhibiting a sublinear dependence in the dimension d , corresponds to the bound that would be obtained if $\Sigma^{-1/2}$ were known (it is then derived by means of the arguments used to study the concentration properties of the empirical halfspace depth, see chapter 26 in [Shorack & Wellner \(1986\)](#)). The upper confidence bound in assertion (ii) differs from that in assertion (i) in two respects. First, the additional terms clearly show the effect of the Monte Carlo approximation, which is negligible when $n \gg m$. Second, the maximal deviation is taken over a compact subset of \mathbb{R}^d . Furthermore, our theoretical analysis can be easily extended to the deviations of the sample version of IRW by simply omitting the term involving the square root of the precision matrix corresponding to the first term of (i) and the last term of (ii) leading to faster rates (see Section B.4 in the Appendix section).

A limited confidence interval. The proof of the assertion (i) relies on controlling the deviations between the eigenvectors (resp., the inverses of the square-root eigenvalues) of $\widehat{\Sigma}$ and those of the true covariance matrix. The lower bound of the δ -range results from this control and is not limiting in practice since it decreases exponentially fast when the sample size increases.

About the constants. Both upper bounds are provided with explicit constants. The explicit linear dependence on the dimension d is due to the operator norm that appears in the proof when controlling the eigenvectors of $\widehat{\Sigma} - \Sigma$. It implies an additional square root of d in the constant Δ following the classical inequality $\|A\|_{\text{op}} \leq \sqrt{d} \|A\|_1$ for any matrix $A \in \mathbb{R}^{d \times d}$ of full rank d . However, Lipschitz constants

L_P and L_R , that are mandatory in order to derive bounds uniformly on \mathbb{R}^d (or \mathcal{B}_r), appear to exhibit an implicit dependence on the dimension d . Indeed, these constants can be derived for r.v. valued in a compact support with bounded density exhibiting an exponential dependence on d . Unfortunately, this concern cannot be avoided unless removing the supremum involved in (i) and (ii). While the depth value at a single point $x \in \mathbb{R}^d$ is usually of limited importance, it is often more relevant in practice that an ensemble of depth values, i.e. the set $\{D(x, P), x \in \mathbb{R}^d\}$, are simultaneously well approximated by their empirical versions for comparison purposes. This implies estimation guarantees for the ranks induced by the depth function when computed on the whole sample X_1, \dots, X_n , on which several applications such as anomaly detection fully rely on. The eigengap γ appears in the denominator due to the use of a variant of the Davis-Kahan theorem (Davis & Kahan, 1970), so as to control the deviations between the eigenvectors of $\hat{\Sigma}$ and those of Σ , and can not be avoided. Observe that both upper-bounds explode as γ or ε vanish. These constants, related to the covariance matrix estimation, are often small in practice (see the Appendix where they are computed on the benchmarked datasets used in Section 5). However, they are often negligible w.r.t. the lipschitz constant in the numerator that is $O(e^d)$ as mentioned above and is thus not limiting.

On optimality. In absence of lower bound (and to the best of our knowledge, no such result is documented in the statistical depth literature yet), the optimality of the bounds above cannot be claimed of course. However, the proof partly consists in bounding the risk of the estimator of the covariance matrix Σ and involves the estimation rates given in Lemma A.5 in the Appendix, which are known to be optimal for sub-Gaussian distributions (Vershynin, 2012). Recall incidentally that has been shown that faster rates for the estimation of the inverse of the covariance matrix can be established under additional sparsity assumptions (see e.g. Theorem 5 in Cai et al. (2010)).

Choosing m . The difficulty of approximating an integral over \mathbb{R}^d by means of Monte-Carlo techniques grows with d . Our theoretical results, such as the upper bound in (ii), shed light on the behaviour of m w.r.t. the dimension d . Indeed, focusing on the term $4L_P/(3m)$, L_P can be explicitated for density bounded distributions involving the volume of the unit sphere \mathbb{S}^{d-1} that depends exponentially on d (see the paragraph above Theorem 4.5). Thus, m should be higher than $O(e^d)$ to yield a good statistical approximation. However, in practice, since computation times depend on m , a trade-off between statistical accuracy (the higher m , the better) and computational burden (the higher m , the heavier) must be found in practice, see Section 5.

Remark 4.6. (RELATED WORK) *We point out that nonasymptotic results about the accuracy of sample versions of statistical depths, such as those stated above, are*

seldom in the literature. To the best of our knowledge, rate bounds have only been derived in the halfspace depth case before. The first result (see Shorack & Wellner (1986) chapter 26), where uniform rates of the sample version are provided, uses the fact that the set of halfspaces in \mathbb{R}^d is of finite VC dimension. Recently, this result has been refined under the Assumptions 4.3 and 4.4 in Burr & Fabrizio (2017). Asymptotic rates of convergence for the Monte Carlo approximation of the halfspace depth, i.e., when the minimum over the unit hypersphere is approximated from a finite number of directions, have been recently established in Nagy et al. (2020). In contrast to the finite-sample framework, uniform asymptotic rates have been proved in several settings. Unfortunately, approximating a minimum over the unit sphere \mathbb{S}^{d-1} using a Monte Carlo scheme is not optimal. Indeed when the distribution is assumed to belong to a bounded subset of \mathbb{R}^d with bounded density, the authors obtain slow rates of order $O((\log(m)/m)^{1/(d-1)})$ suffering from the curse of dimensionality. Furthermore, they show that obtaining uniform rates of the halfspace depth approximation is not possible in absence of the bounded density assumption, see Section 4.2 in Nagy et al. (2020).

5. Numerical Experiments

The advantages of the novel notion of depth introduced in Section 3 are supported by various experimental results in this part. First, we explore empirically the behavior of the returned ranks as the number of sampled projections increases. Second, the application of the AI-IRW depth to anomaly detection is considered, illustrating clearly the improvement on the performance attained. Due to space limitations, additional experiments are provided in the Appendix.

On approximating the AI-IRW depth. The accuracy of Monte Carlo approximation, depending on the number m of random directions uniformly sampled, is evaluated for the empirical versions of the AI-IRW depth. A robust estimator of the AI-IRW is also introduced using the well-known Minimum Covariance Determinant (MCD) estimator (Rousseeuw, 1984) of the covariance matrix. The experiment is based on samples of size $n = 1000$ drawn from a centered Gaussian distribution with covariance matrix sampled from a Wishart distribution (with parameters (d, \mathcal{I}_d)), where the dimension d varies in the range $\{2, 5, 10, 15, 20, 30, 40, 50\}$. We compute $\tilde{D}_{\text{AI-IRW}}^{\text{MC}}$ on these samples by varying the number of projections m between 100 and 7000. As AI-IRW does not possess any closed-form, we propose to evaluate the quality of the returned ranks considering $\tilde{D}_{\text{AI-IRW}}^{\text{MC}}$ computed with $m = 200000$ projections as the “true” depth. The coherence between ranks is assessed using the popular Kendall τ correlation coefficient, see Kendall (1938). This whole procedure is repeated 10 times and the averaged results are reported in Figure 2. As

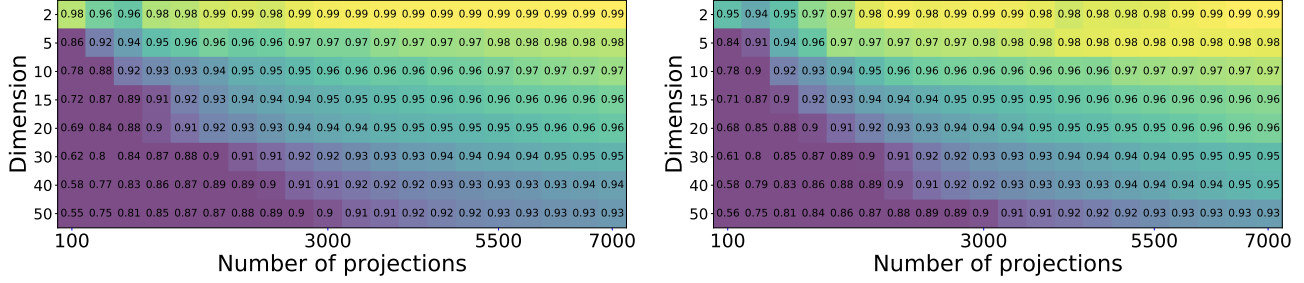


Figure 2. Kendall correlation between the approximated ranks of AI-IRW and their true ranks using SC (left) and MCD estimates (right) depending on the number of approximating projections m for a Gaussian distribution.

expected, the quality of the approximation increases with m and decreases with d . Interestingly, sharp approximations are obtained with far less than $O(e^d)$ projections. Indeed, in the worst case, i.e. when $d = 50$, a correlation of 0.93 is attained for AI-IRW, using both sample covariance (SC) and MCD (with support fraction set to $(n+d+1)/2$) estimators, with only 5500 directions which is roughly $100 \times d$ while $e^{50} \approx 10^{21}$. In low dimension, few projections are needed to obtain correlation higher than 0.98. In view of these results and because of the computation time of the approximations (documented in Section D.2 of the Appendix due to space constraints), choosing $m = 100d$ appears as a good compromise between statistical accuracy and computation time, as done in the next experiment.

Application to anomaly detection. To illustrate the performance improvement due to introduction of affine invariance to the IRW, we conduct a comprehensive comparative study of anomaly detection on 10 widely used data sets in the literature¹: *Mulcross*, *Shuttle*, *Thyroid*, *Wine*, *Http*, *Smtip*, *Ecoli*, *Breastw*, *Musk* and *Satimage* varying in size and dimension. In this unsupervised setting (we train all methods on unlabeled data), we use labels only to assess the performance of the methods by Area Under the Receiver Operation Characteristic curve (AUROC). We contrast the proposed approach with the non affine-invariant version, the original halfspace depth (T), halfspace mass depth (HM) (Chen et al., 2015), the AutoEncoder (AE) (Aggarwal, 2015) where the reconstruction error is used as anomaly score and one of the most used multivariate anomaly detection algorithms: Isolation Forest (IF) (Liu et al., 2008; Staerman et al., 2019). The performance of these methods being relatively insensitive to their parameters, they are set by default. Based on the previous experiment, AI-IRW, IRW, and halfspace depths are calibrated with $m = 100 \times d$. From Table 1 one observes that AI-IRW uniformly (and significantly in many cases) improves on standard IRW that is rather comparable with Isolation Forest and the halfspace mass depth. Additional information on the data sets as well as the computation time

are given in Section D.3.2 in the Appendix.

	AI-IRW	IRW	HM	T	IF	AE
Ecoli	0.85	0.83	0.88	0.68	0.77	0.64
Shuttle	0.99	0.99	0.99	0.86	0.99	0.99
Mulcross	1	0.98	1	0.87	0.96	1
Thyroid	0.98	0.80	0.84	0.92	0.97	0.97
Wine	0.96	0.96	0.99	0.71	0.8	0.72
Http	1	0.95	0.97	0.99	1	1
Smtip	0.96	0.77	0.74	0.85	0.90	0.82
Breastw	0.97	0.97	0.99	0.84	0.99	0.91
Musk	1	0.84	0.97	0.77	1	1
Satimage	0.99	0.96	0.98	0.95	0.99	0.98

Table 1. AUROCs of benchmarked anomaly detection methods.

6. Conclusion

In this paper, we have introduced a novel notion of statistical depth (AI-IRW), modifying the original Integrated Rank-Weighted (IRW) depth proposal in Ramsay et al. (2019). It has been shown that the AI-IRW depth does not only inherit all the compelling features of the IRW depth, its theoretical properties and its computational advantages (no optimization problem solving is required to compute it), but also fulfills in addition the affine invariance property, crucial regarding interpretability/reliability issues. The natural idea at work consists in averaging univariate Tukey halfspace depths computed from random projections of the data onto (nearly) uncorrelated lines, defined by the (empirical) covariance structure of the data, rather than projections onto lines fully generated at random. Though the AI-IRW sample version exhibits a complex probabilistic structure, an estimator of the precision matrix being involved in its definition, a nonasymptotic analysis has been carried out here, revealing its good concentration properties around the true AI-IRW depth. The merits of the AI-IRW depth have been illustrated by encouraging numerical experiments, for anomaly detection purpose in particular, offering the perspective of a widespread use for various statistical learning tasks.

¹<http://odds.cs.stonybrook.edu/>

Acknowledgements

This work has been funded by BPI France in the context of the PSPC Project Espresso (2017-2021).

References

- Aggarwal, C. C. Outlier analysis. *Data Mining*, 2015.
- Burr, M. A. and Fabrizio, R. J. Uniform convergence rates for halfspace depth. *Statistics and Probability Letters*, 124:33 – 40, 2017.
- Cai, T. T. and Zhou, H. H. Optimal rates of convergence for sparse covariance matrix estimation. *The Annals of Statistics*, 40(5):2389–2420, 2013.
- Cai, T. T., Zhang, C.-H., and Zhou, H. H. Optimal rates of convergence for covariance matrix estimation. *The Annals of Statistics*, 38(4):2118–2144, 2010.
- Chaudhuri, P. On a geometric notion of quantiles for multivariate data. *Journal of the American Statistical Association*, 91(434):862–872, 1996.
- Chen, B., Ting, K. M., Washio, T., and Haffari, G. Halfspace mass: a maximally robust and efficient data depth method. *Machine Learning*, 100(2):677–699, 2015.
- Chen, Y., Wiesel, A., Eldar, Y. C., and Hero, A. O. Shrinkage algorithms for mmse covariance estimation. *IEEE Transactions on Signal Processing*, 58(10):5016–5029, 2010.
- Chernozhukov, V., Galichon, A., Hallin, M., and Henry, M. Monge–kantorovich depth, quantiles, ranks and signs. *The Annals of Statistics*, 45(1):223–256, 02 2017.
- Cuevas, A. and Fraiman, R. On depth measures and dual statistics. a methodology for dealing with general data. *Journal of Multivariate Analysis*, 100(4):753–766, 2009.
- Davis, C. and Kahan, W. M. The rotation of eigenvectors by a perturbation. *SIAM Journal on Numerical Analysis*, 7(1):1–46, 1970.
- Donoho, D. L. *Breakdown Properties of Multivariate Location Estimators*. PhD thesis, Harvard University, 1982.
- Donoho, D. L. and Gasko, M. Breakdown properties of location estimates based on halfspace depth and projected outlyingness. *The Annals of Statistics*, 20:1803–1827, 1992.
- Dyckerhoff, R. Data depths satisfying the projection property. *ASTA - Advances in Statistical Analysis*, 88(2):163–190, 2004.
- Dyckerhoff, R., Mozharovskyi, P., and Nagy, S. Approximate computation of projection depths. *Computational Statistics & Data Analysis*, 157(C), 2021.
- Einmahl, J. H., Li, J., and Liu, R. Y. Bridging centrality and extremity: Refining empirical data depth using extreme value statistics. *The Annals of Statistics*, 43(6):2738–2765, 12 2015.
- Fan, J., Liao, Y., and Liu, H. An overview of the estimation of large covariance and precision matrices. *The Econometrics Journal*, 19(1):C1–C32, 2016.
- Friedman, J., Hastie, T., and Tibshirani, R. Sparse inverse covariance estimation with the graphical lasso. *Biostatistics*, 9(3):432–441, 2008.
- Kalos, M. H. and Whitlock, P. A. *Monte Carlo Methods*. Wiley-Blackwell, 2008.
- Kendall, M. G. A new measure of rank correlation. *Biometrika*, 30(1/2):81–93, 1938.
- Koshevoy, G. and Mosler, K. Zonoid trimming for multivariate distributions. *The Annals of Statistics*, 25(5):1998–2017, 10 1997.
- Koshevoy, G. A. The Tukey depth characterizes the atomic measure. *Journal of Multivariate Analysis*, 83:360–364, 2002.
- Krantz, S. G. and Parks, H. R. *Geometric Integration Theory*. Birkhäuser, 2008.
- Ledoit, O. and Wolf, M. A well-conditioned estimator for large-dimensional covariance matrices. *Journal of Multivariate Analysis*, 88(2):365–411, 2004.
- Liu, F. T., Ting, K. M., and Zhou, Z.-H. Isolation forest. In *2008 Eighth IEEE International Conference on Data Mining*, 2008.
- Liu, R. Y. On a notion of data depth based upon random simplices. *The Annals of Statistics*, 1990.
- Liu, R. Y. *Data Depth and Multivariate Rank Tests*, pp. 279–294. North-Holland, Amsterdam, 1992.
- Liu, R. Y. and Singh, K. A quality index based on data depth and multivariate rank tests. *Journal of the American Statistical Association*, 88(421):252–260, 1993.
- Liu, X. and Zuo, Y. Computing halfspace depth and regression depth. *Communications in Statistics - Simulation and Computation*, 2014.
- Liu, X., Mosler, K., and Mozharovskyi, P. Fast computation of tukey trimmed regions and median in dimension $p > 2$. *Journal of Computational and Graphical Statistics*, 2018. in press.

- Mosler, K. Depth statistics. In Becker, C., Fried, R., and Kuhnt, S. (eds.), *Robustness and Complex Data Structures: Festschrift in Honour of Ursula Gather*, pp. 17–34. Springer, 2013.
- Nagy, S., Dyckerhoff, R., and Mozharovskiy, P. Uniform convergence rates for the approximated halfspace and projection depth. *Electronic Journal of Statistics*, 14(2): 3939 – 3975, 2020.
- Oja, H. Descriptive statistics for multivariate distributions. *Statistics & Probability Letters*, 1(6):327 – 332, 1983.
- Pedregosa, F., Varoquaux, G., Gramfort, A., Michel, V., Thirion, B., Grisel, O., Blondel, M., Prettenhofer, P., Weiss, R., Dubourg, V., Vanderplas, J., Passos, A., Cournapeau, D., Brucher, M., Perrot, M., and Duchesnay, E. Scikit-learn: Machine learning in Python. *Journal of Machine Learning Research*, 12:2825–2830, 2011.
- Ramsay, K., Durocher, S., and Leblanc, A. Integrated rank-weighted depth. *Journal of Multivariate Analysis*, 173: 51–69, 2019.
- Rousseeuw, P. J. Least median of squares regression. *Journal of the American Statistical Association*, 79(388):871–880, 1984.
- Rousseeuw, P. J. and Struyf, A. Computing location depth and regression depth in higher dimensions. *Statistics and Computing*, 8(3):193–203, 1998.
- Rousseeuw, P. J. and van Driessen, K. A fast algorithm for the minimum covariance determinant estimator. *Technometrics*, 41(3):212–223, 1999.
- Schäfer, J. and Strimmer, K. A shrinkage approach to large-scale covariance matrix estimation and implications for functional genomics. *Statistical applications in genetics and molecular biology*, 4(32), 2005.
- Shorack, G. R. and Wellner, J. A. *Empirical Processes with Applications to Statistics*. John Wiley & Sons, 1986.
- Staerman, G., Mozharovskiy, P., Cléménçon, S., and d’Alché Buc, F. Functional isolation forest. In *Proceedings of The Eleventh Asian Conference on Machine Learning*, volume 101, pp. 332–347, 2019.
- Struyf, A. and Rousseeuw, P. Halfspace depth and regression depth characterize the empirical distribution. *Journal of Multivariate Analysis*, 69:135–153, 1999.
- Tukey, J. W. Mathematics and the picturing of data. In James, R. (ed.), *Proceedings of the International Congress of Mathematicians*, volume 2, pp. 523–531, 1975.
- Vardi, Y. and Zhang, C.-H. The multivariate 11-median and associated data depth. *Proceedings of the National Academy of Sciences*, 97(4):1423–1426, 2000.
- Vershynin, R. How close is the sample covariance matrix to the actual covariance matrix? *Journal of Theoretical Probability*, 25(3):655–686, 2012.
- Wedin, P.-A. Perturbation theory for pseudo-inverses. *IT Numerical Mathematics*, 1973.
- Weyl, H. Das asymptotische verteilungsgesetz der eigenwerte linearer partieller differentialgleichungen. *Mathematische Annalen*, 71(4):441–479, 1912.
- Yu, Y., Wang, T., and Samworth, R. J. A useful variant of the Davis–Kahan theorem for statisticians. *Biometrika*, 102(2):315–323, 2014.
- Zhang, J. Some extensions of tukey’s depth function. *Journal of Multivariate Analysis*, 82(1):134–165, 2002.
- Zhao, Y., Nasrullah, Z., and Li, Z. Pyod: A python toolbox for scalable outlier detection. *Journal of Machine Learning Research*, 20(96):1–7, 2019.
- Zuo, Y. Projection-based depth functions and associated medians. *The Annals of Statistics*, 31(5):1460–1490, 2003.
- Zuo, Y. and Serfling, R. General notions of statistical depth function. *The Annals of Statistics*, 28(2):461–482, 2000.

This Appendix is organized as follows.

- Useful preliminary results are stated and proved in Appendix A.
- The proofs of the results stated in the paper are given in Appendix B.
- The approximation algorithm to compute the AI-IRW depth is described in Appendix C.
- Additional experiments are displayed in Appendix D.

A. Preliminary Results

First, we recall some lemmas on linear algebra, halfspace depth and covariance matrix estimation, used in the subsequent proofs.

A.1. Basics of Linear Algebra

Here useful results of linear algebra are recalled for clarity.

Lemma A.1 (Wedin (1973), Theorem 4.1). *Let A and B be two invertible matrices of size $d \times d$ and $\|A\|_{\text{op}}$ be the operator norm of matrix A . Then it holds:*

$$\|A^{-1} - B^{-1}\|_{\text{op}} \leq \|A^{-1}\|_{\text{op}} \|B^{-1}\|_{\text{op}} \|A - B\|_{\text{op}}. \quad (7)$$

Lemma A.2 (Vershynin (2012), Lemma 2.2). *Let A be a matrix of size $d \times d$ and N_ρ be an ρ -net of \mathbb{S}^{d-1} . Then it holds:*

$$\|A\|_{\text{op}} \leq \frac{1}{1 - 2\rho} \max_{v \in N_\rho} |v^\top A v|.$$

Lemma A.3. *Let A_1 and A_2 be two real symmetric and invertible matrices of dimension $d \times d$ with $O_1 D_1 O_1^\top$ and $O_2 D_2 O_2^\top$ their eigenvalues decomposition in orthonormal bases. Then it holds:*

$$\|A_1^{-1/2} - A_2^{-1/2}\|_{\text{op}} \leq \|D_2^{-1/2}\|_{\text{op}} \left(\|D_1^{1/2} - D_2^{1/2}\|_{\text{op}} \|D_1^{-1/2}\|_{\text{op}} + \|O_1 - O_2\|_{\text{op}} \right).$$

Proof.

$$\begin{aligned} \|O_1 D_1^{-1/2} - O_2 D_2^{-1/2}\|_{\text{op}} &\leq \|O_1\|_{\text{op}} \|D_1^{-1/2} - D_2^{-1/2}\|_{\text{op}} + \|O_1 - O_2\|_{\text{op}} \|D_2^{-1/2}\|_{\text{op}} \\ &\leq \|D_1^{-1/2} - D_2^{-1/2}\|_{\text{op}} + \|D_2^{-1/2}\|_{\text{op}} \|O_1 - O_2\|_{\text{op}} \\ &\stackrel{(i)}{\leq} \|D_2^{-1/2}\|_{\text{op}} \left(\|D_1^{1/2} - D_2^{1/2}\|_{\text{op}} \|D_1^{-1/2}\|_{\text{op}} + \|O_1 - O_2\|_{\text{op}} \right), \end{aligned}$$

where (i) holds due to Lemma A.1. □

A.2. Non-Asymptotic Rates on Halfspace Depth and Sample Covariance Matrix

We now recall useful results on maximum deviations of the halfspace depth estimator as well as the sample covariance matrix.

Lemma A.4 (Shorack & Wellner (1986), Chapter 26). *Let $P \in \mathcal{P}(\mathbb{R}^d)$. Let X_1, \dots, X_n a sample from P with empirical measure $\hat{P} = (1/n) \sum_{i=1}^n \delta_{X_i}$. Denote by F_u and \hat{F}_u the cdf of P_u and \hat{P}_u respectively. Then, for any $t > 0$, it holds:*

$$\mathbb{P} \left(\sup_{\substack{x \in \mathbb{R}^d \\ u \in \mathbb{S}^{d-1}}} \left| \hat{F}_u(u^\top x) - F_u(u^\top x) \right| > t \right) \leq \frac{6(2n)^{d+1}}{(d+1)!} \exp(-nt^2/8).$$

Lemma A.5 (Variant of [Vershynin \(2012\)](#), Proposition 2.1). *Let Σ be the covariance matrix of a τ sub-Gaussian random variables X that takes its values in \mathbb{R}^d . Let X_1, \dots, X_n be a sample from X and denote by $\widehat{\Sigma} = \frac{1}{n} \sum_{i=1}^n X_i X_i^\top$ the SC estimator of Σ . Then it holds:*

$$\mathbb{P} \left(\|\widehat{\Sigma} - \Sigma\|_{\text{op}} > t \right) \leq 2 \times 9^d \exp \left\{ -\frac{n}{2} \min \left\{ \frac{t^2}{(32\tau^2)^2}, \frac{t}{32\tau^2} \right\} \right\}.$$

Let $\sigma_d > \dots > \sigma_1$ and $\widehat{\sigma}_d > \dots > \widehat{\sigma}_1$ be respectively the ordered eigenvalues of Σ and $\widehat{\Sigma}$. Using [Weyl's Theorem \(1912\)](#), it holds:

$$\mathbb{P} \left(\max_{1 \leq k \leq d} |\widehat{\sigma}_k - \sigma_k| > t \right) \leq 2 \times 9^d \exp \left\{ -\frac{n}{2} \min \left\{ \frac{t^2}{(32\tau^2)^2}, \frac{t}{32\tau^2} \right\} \right\}.$$

Proof. Let N_ρ be an ρ -net of the sphere \mathbb{S}^{d-1} . Applying [Lemma A.2](#) on $\widehat{\Sigma} - \Sigma$, for any $t, \rho > 0$, we have

$$\begin{aligned} \mathbb{P} \left(\|\widehat{\Sigma} - \Sigma\|_{\text{op}} > t \right) &\leq \mathbb{P} \left(\frac{1}{1-2\rho} \max_{v \in N_\rho} |v^\top (\widehat{\Sigma} - \Sigma)v| > t \right) \\ &\leq |N_\rho| \mathbb{P} \left(|v^\top (\widehat{\Sigma} - \Sigma)v| > (1-2\rho)t \right), \end{aligned}$$

where $|N_\rho|$ stands for the cardinal of the set N_ρ . Noticing that $\widehat{\Sigma} = \frac{1}{n} \sum_{i=1}^n X_i X_i^\top$ is a sum of independent matrices we have

$$v^\top (\widehat{\Sigma} - \Sigma)v = \frac{1}{n} \sum_{i=1}^n Z_i - \mathbb{E}Z_i,$$

where $Z_i = (v^\top X_i)^2$ for every $1 \leq i \leq n$ and $Z_i - \mathbb{E}Z_i$ are i.i.d random variables that are $((16\tau)^2, 16\tau^2)$ sub-exponential. Choosing $\rho = 1/4$, noticing that $|N_{1/4}| \leq 9^d$ and applying the sub-exponential tail bound lead to the desired result. \square

A.3. Affine-Invariance is not fulfilled by IRW in general

Here we provide an example of discrete distribution where IRW does not satisfy affine-invariance property.

Consider the discrete probability measure P assigning the weight $1/3$ to the bivariate points in $\mathcal{D}_3 = \{(-1, 2), (3, 3), (2, 1)\}$ and let us compute the IRW depth of $x = (0, 1)$ and $y = (3, 2)$ relative to P . It is easy to see that the mappings $u \in \mathbb{S}^1 \mapsto D_{H,1}(\langle u, x \rangle, P_u)$ and $u \in \mathbb{S}^1 \mapsto D_{H,1}(\langle u, y \rangle, P_u)$ take only two values, 0 or $1/3$. Identifying \mathbb{S}^1 as $[0, 2\pi[$, the univariate halfspace depth of x relative to P is then null for any $u \in [\pi/4, \pi/2] \cup [5\pi/4, 3\pi/2]$ and equal to $1/3$ if u belongs to the complementary set. In addition, $D_{H,1}(\langle u, y \rangle, P_u)$ is equal to 0 for any $u \in [3\pi/4, \pi] \cup [7\pi/4, 2\pi]$ and equal to $1/3$ on the complementary set. One may easily check that $D_{\text{IRW}}(x, P) = D_{\text{IRW}}(y, P) = 0.25$ and the same rank would be then assigned to each point by the IRW depth. Now, multiplying all ordinate values by 2, which is an affine transformation, the univariate halfspace depth of $\tilde{x} = (0, 2)$ is now null for all u in $[\pi/8, \pi/2] \cup [9\pi/8, 3\pi/2]$ while it remains equal to $1/3$ on the complementary set of this region. The depth of \tilde{x} is thus lower than 0.25. On the other hand, the univariate depth of $\tilde{y} = (3, 4)$ is now null on $[7\pi/8, \pi] \cup [15\pi/8, 2\pi]$ while it remains equal to $1/3$ on the complementary set of this interval. It follows that $D_{\text{IRW}}(\tilde{x}) = 5/24 < 0.25 < 7/24 = D_{\text{IRW}}(\tilde{y})$.

B. Technical Proofs of the Main Results

We now prove the main results stated in the paper.

B.1. Proof of Proposition 3.2

B.1.1. AFFINE-INVARIANCE

Let $A \in \mathbb{R}^{d \times d}$ be a non singular matrix and $b \in \mathbb{R}^d$. Let Σ_X and Σ_{AX} the covariance matrix of X and AX respectively. Defines the Cholesky decomposition as $\Sigma_X = \Lambda_X \Lambda_X^\top$ and $\Sigma_{AX} = A \Lambda_X \Lambda_X^\top A^\top = \Lambda_{AX} \Lambda_{AX}^\top$. It holds:

$$\begin{aligned}
 D_{\text{AI-IRW}}(Ax + b, AX + b) &= \frac{1}{V_d} \int_{\mathbb{S}^{d-1}} D_{\text{H},1}(\langle \frac{\Lambda_{AX+b}^{-\top} u}{\|\Lambda_{AX+b}^{-\top} u\|}, Ax + b \rangle, \langle \frac{\Lambda_{AX+b}^{-\top} u}{\|\Lambda_{AX+b}^{-\top} u\|}, AX + b \rangle) du \\
 &= \frac{1}{V_d} \int_{\mathbb{S}^{d-1}} D_{\text{H},1}(\langle \Lambda_{AX+b}^{-\top} u, Ax + b \rangle, \langle \Lambda_{AX+b}^{-\top} u, AX + b \rangle) du \\
 &= \frac{1}{V_d} \int_{\mathbb{S}^{d-1}} D_{\text{H},1}(\langle \Lambda_{AX}^{-\top} u, Ax \rangle, \langle \Lambda_{AX}^{-\top} u, AX \rangle) du \\
 &= \frac{1}{V_d} \int_{\mathbb{S}^{d-1}} D_{\text{H},1}(\langle u, \Lambda_X^{-1} x \rangle, \langle u, \Lambda_X^{-1} X \rangle) du \\
 &= \frac{1}{V_d} \int_{\mathbb{S}^{d-1}} D_{\text{H},1}(\langle \frac{\Lambda_X^{-\top} u}{\|\Lambda_X^{-\top} u\|}, x \rangle, \langle \frac{\Lambda_X^{-\top} u}{\|\Lambda_X^{-\top} u\|}, X \rangle) du \\
 &= D_{\text{AI-IRW}}(x, P).
 \end{aligned}$$

The same reasoning applies if the square matrix is given by the SVD decomposition.

B.1.2. PROOF OF MAXIMALITY AT THE CENTER

Assume that P is halfspace symmetric about a unique β , i.e., $\mathbb{P}(X \in \mathcal{H}_\beta) \geq \frac{1}{2}$ for every closed halfspace \mathcal{H}_β such that $\beta \in \partial \mathcal{H}$ with $\partial \mathcal{H}$ the boundary of \mathcal{H} . Thus, it is easy to see that $D_{\text{AI-IRW}}(\beta, P) \geq \frac{1}{2}$. The uniqueness of β and the fact that $D_{\text{AI-IRW}}$ is lower than $1/2$ for any element in \mathbb{R}^d by definition imply that

$$\beta = \operatorname{argsup}_{x \in \mathbb{R}^d} D_{\text{AI-IRW}}(x, P).$$

B.1.3. VANISHING AT INFINITY

The proof is a particular case of the proof of theorem 1 in Cuevas & Fraiman (2009). We detail it for the sake of clarity. Let U be a random variable following ω_{d-1} , the uniform measure on the unit sphere \mathbb{S}^{d-1} . Defines $V = \Sigma^{-\top/2} U / \|\Sigma^{-\top/2} U\|$ and ν_{d-1} its probability distribution. Let $\theta > 0$ and $x \in \mathbb{R}^d$, then $r(\theta) := \nu_{d-1}\{v : \frac{|\langle v, x \rangle|}{\|x\|} \leq \theta\}$ goes to zero when $\theta \rightarrow 0$. For any $x \in \mathbb{R}_{\setminus\{0\}}^d$, we have

$$\begin{aligned}
 D_{\text{AI-IRW}}(x, P) &= \int_{\mathbb{R}^d} \min \{F_v(v^\top x), 1 - F_v(v^\top x)\} d\nu_{d-1}(v) \\
 &\leq \int_{\mathbb{R}^d} \mathbb{I} \left\{ v : \frac{|\langle v, x \rangle|}{\|x\|} \leq \theta \right\} d\nu_{d-1}(v) \\
 &+ \int_{\mathbb{R}^d} F_v(v^\top x) \mathbb{I} \left\{ v : \frac{|\langle v, x \rangle|}{\|x\|} > \theta, \langle v, x \rangle \leq 0 \right\} d\nu_{d-1}(v) \\
 &+ \int_{\mathbb{R}^d} (1 - F_v(v^\top x)) \mathbb{I} \left\{ v : \frac{|\langle v, x \rangle|}{\|x\|} > \theta, \langle v, x \rangle > 0 \right\} d\nu_{d-1}(v) \\
 &\leq r(\theta) + \int_{\mathbb{R}^d} F_v(-\theta \|x\|) \mathbb{I} \left\{ v : \frac{|\langle v, x \rangle|}{\|x\|} > \theta, \langle v, x \rangle \leq 0 \right\} d\nu_{d-1}(v) \\
 &+ \int_{\mathbb{R}^d} (1 - F_v(\theta \|x\|)) \mathbb{I} \left\{ v : \frac{|\langle v, x \rangle|}{\|x\|} > \theta, \langle v, x \rangle > 0 \right\} d\nu_{d-1}(v).
 \end{aligned}$$

Now, when $\|x\| \rightarrow \infty$, the dominated convergence theorem ensures that

$$\lim_{\|x\| \rightarrow \infty} \sup_{\theta \rightarrow 0} D_{\text{AI-IRW}}(x, P) \leq r(\theta) \rightarrow 0.$$

B.1.4. DECREASING ALONG RAYS

The proof is a slight modification of the proof of Assertion (iii) of Theorem 2 in Ramsay et al. (2019). Details are left to the reader.

B.1.5. CONTINUITY

For any $P \in \mathcal{P}(\mathbb{R}^d)$, the continuity of the inner product and the cdf ensure continuity of $D_H(v^\top x, v^\top X)$ for any $v \in \mathbb{S}^{d-1}$. Therefore, the continuity of $x \mapsto D_{\text{AI-IRW}}(x, P)$ follows from dominated convergence.

B.2. Proof of Theorem 4.5

We now prove the main results of the paper.

B.2.1. ASSERTION (I)

Introducing terms and using triangle inequality, it holds:

$$\sup_{x \in \mathbb{R}^d} \left| \widehat{D}_{\text{AI-IRW}}(x) - D_{\text{AI-IRW}}(x, P) \right| \leq \underbrace{\sup_{x \in \mathbb{R}^d} \left| \widehat{F}_{\widehat{V}}(\widehat{V}^\top x) - F_{\widehat{V}}(\widehat{V}^\top x) \right|}_{(1)} + \underbrace{\sup_{x \in \mathbb{R}^d} \left| F_{\widehat{V}}(\widehat{V}^\top x) - F_V(V^\top x) \right|}_{(2)}.$$

Now, the first term (1) can be controlled using the bound for the deviations of halfspace depth deferred in Lemma A.4. Thus, for any $t > 0$ it holds:

$$\begin{aligned} \mathbb{P} \left(\sup_{x \in \mathbb{R}^d} \left| \widehat{F}_{\widehat{V}}(\widehat{V}^\top x) - F_{\widehat{V}}(\widehat{V}^\top x) \right| > t/2 \right) &\leq \mathbb{P} \left(\sup_{\substack{y \in \mathbb{R}^d \\ u \in \mathbb{S}^{d-1}}} \left| \widehat{F}_u(u^\top y) - F_u(u^\top y) \right| > t/2 \right) \\ &\leq \frac{6(2n)^{d+1}}{(d+1)!} \exp(-nt^2/32). \end{aligned} \quad (8)$$

The second term (2) relies on the influence of the deviations of the sample covariance matrix. First remark that:

$$\begin{aligned} \sup_{x \in \mathbb{R}^d} \left| F_{\widehat{V}}(\widehat{V}^\top x) - F_V(V^\top x) \right| &\leq \sup_{\substack{x \in \mathbb{R}^d \\ u \in \mathbb{S}^{d-1}}} \left| \mathbb{P} \left(\left\langle \frac{\widehat{\Sigma}^{-\top/2} u}{\|\widehat{\Sigma}^{-\top/2} u\|}, X - x \right\rangle \leq 0 \mid \mathcal{S}_n \right) \right. \\ &\quad \left. - \mathbb{P} \left(\left\langle \frac{\Sigma^{-\top/2} u}{\|\Sigma^{-\top/2} u\|}, X - x \right\rangle \leq 0 \right) \right|. \end{aligned}$$

Now, since X is radially Lipschitz continuous, we have:

$$\left| \mathbb{P} \left(\left\langle \frac{\widehat{\Sigma}^{-\top/2} u}{\|\widehat{\Sigma}^{-\top/2} u\|}, X - x \right\rangle \leq 0 \mid \mathcal{S}_n \right) - \mathbb{P} \left(\left\langle \frac{\Sigma^{-\top/2} u}{\|\Sigma^{-\top/2} u\|}, X - x \right\rangle \leq 0 \right) \right| \leq L_R \left\| \frac{\widehat{\Sigma}^{-\top/2} u}{\|\widehat{\Sigma}^{-\top/2} u\|} - \frac{\Sigma^{-\top/2} u}{\|\Sigma^{-\top/2} u\|} \right\|.$$

Introducing terms and using triangle inequality leads to:

$$\begin{aligned} \left\| \frac{\widehat{\Sigma}^{-\top/2} u}{\|\widehat{\Sigma}^{-\top/2} u\|} - \frac{\Sigma^{-\top/2} u}{\|\Sigma^{-\top/2} u\|} \right\| &\leq \frac{\|\widehat{\Sigma}^{-1/2} - \Sigma^{-1/2}\|_{\text{op}}}{\|\Sigma^{-1/2} u\|} + \|\widehat{\Sigma}^{-1/2} u\| \left(\frac{1}{\|\widehat{\Sigma}^{-1/2} u\|} - \frac{1}{\|\Sigma^{-1/2} u\|} \right) \\ &\leq \frac{2\|\widehat{\Sigma}^{-1/2} - \Sigma^{-1/2}\|_{\text{op}}}{\|\Sigma^{-1/2} u\|}, \end{aligned}$$

yielding:

$$\sup_{x \in \mathbb{R}^d} \left| F_{\hat{V}}(\hat{V}^\top x) - F_V(V^\top x) \right| \leq \frac{2L_R}{\|\Sigma^{-1/2}\|_{\text{op}}} \|\hat{\Sigma}^{-1/2} - \Sigma^{-1/2}\|_{\text{op}}. \quad (9)$$

Assume that ODO^\top and $\hat{O}\hat{D}\hat{O}^\top$ are the eigenvalues decomposition of Σ and $\hat{\Sigma}$ in orthonormal bases. Thus, thanks to Lemma A.3, we have:

$$\|\hat{\Sigma}^{-1/2} - \Sigma^{-1/2}\|_{\text{op}} \leq \|\Sigma^{-1/2}\|_{\text{op}} \left(\|\hat{D}^{1/2} - D^{1/2}\|_{\text{op}} \|\hat{D}^{-1/2}\|_{\text{op}} + \|\hat{O} - O\|_{\text{op}} \right)$$

Now, since $\min_{k \leq d} \sqrt{\hat{\sigma}_k} \geq \sqrt{\varepsilon} - \max_{k \leq d} |\sqrt{\hat{\sigma}_k} - \sqrt{\sigma_k}|$ and $\max_{k \leq d} |\sqrt{\hat{\sigma}_k} - \sqrt{\sigma_k}| \leq \frac{1}{\sqrt{\varepsilon}} \max_{1 \leq k \leq d} |\hat{\sigma}_k - \sigma_k|$, using Weyl's inequality leads to:

$$\sup_{x \in \mathbb{R}^d} \left| F_{\hat{V}}(\hat{V}^\top x) - F_V(V^\top x) \right| \leq 2L_R \left(\frac{\|\hat{\Sigma} - \Sigma\|_{\text{op}}}{\varepsilon - \|\hat{\Sigma} - \Sigma\|_{\text{op}}} + \|\hat{O} - O\|_{\text{op}} \right).$$

By \mathcal{A}_ξ it is denoted the event $\mathcal{A}_\xi = \left\{ \|\hat{\Sigma} - \Sigma\|_{\text{op}} < \varepsilon - \xi \right\}$ for any $\xi \in [0, \varepsilon)$. Using union bound and combining (9) with the previous equation, for any $t > 0$ and $\xi \in (0, \varepsilon)$ it holds:

$$\begin{aligned} \mathbb{P} \left(\sup_{x \in \mathbb{R}^d} \left| F_{\hat{V}}(\hat{V}^\top x) - F_V(V^\top x) \right| > t/2 \right) &\leq \mathbb{P} \left(\frac{2L_R}{\xi} \|\hat{\Sigma} - \Sigma\|_{\text{op}} > t/4 \right) + \mathbb{P}(\mathcal{A}_\xi^c) \\ &\quad + \mathbb{P} \left(2L_R \|\hat{O} - O\|_{\text{op}} > t/4 \right), \end{aligned}$$

where \mathcal{A}_ξ^c stands for the complementary event of \mathcal{A}_ξ . Applying Lemma A.5 gives:

$$\mathbb{P} \left(\|\hat{\Sigma} - \Sigma\|_{\text{op}} > \frac{\xi t}{8L_R} \right) \leq 2 \times 9^d \exp \left\{ -\frac{n}{2} \min \left\{ \frac{(\xi t)^2}{(256L_R\tau^2)^2}, \frac{\xi t}{256L_R\tau^2} \right\} \right\}, \quad (10)$$

and

$$\mathbb{P}(\mathcal{A}_\xi^c) \leq 2 \times 9^d \exp \left\{ -\frac{n}{2} \min \left\{ \frac{(\varepsilon - \xi)^2}{(32\tau^2)^2}, \frac{\varepsilon - \xi}{32\tau^2} \right\} \right\}. \quad (11)$$

Furthermore, it is easy to see that $\|\hat{O} - O\|_{\text{op}} \leq \sqrt{d} \max_{k \leq d} \|\hat{O}_k - O_k\|$ where O_k is the k -th column of the matrix O . Let γ be the minimum eigengap, following a variant of the Davis-Kahan theorem (Davis & Kahan, 1970) (see corollary 1 in Yu et al. (2014)), it holds:

$$\|\hat{O} - O\|_{\text{op}} \leq \frac{2\sqrt{2d}\|\hat{\Sigma} - \Sigma\|_{\text{op}}}{\gamma}.$$

Using Lemma A.5 again leads to:

$$\mathbb{P} \left(\frac{4L_R\sqrt{2d}\|\hat{\Sigma} - \Sigma\|_{\text{op}}}{\gamma} > t/4 \right) \leq 2 \times 9^d \exp \left\{ -\frac{n}{2} \min \left\{ \frac{(\gamma t)^2}{(512L_R\sqrt{2d}\tau^2)^2}, \frac{\gamma t}{512L_R\sqrt{2d}\tau^2} \right\} \right\}. \quad (12)$$

Combining (10), (11) and (12) it holds:

$$\mathbb{P} \left(\sup_{x \in \mathbb{R}^d} \left| F_{\hat{V}}(\hat{V}^\top x) - F_V(V^\top x) \right| > t/2 \right) \leq 6 \times 9^d \exp \left(-\frac{n}{2} \min \left\{ (\kappa t)^2, \kappa t \right\} \right),$$

for any $t \leq (\varepsilon - \xi)/(32\tau^2\kappa)$ where $\kappa = \frac{1}{256L_R\tau^2} \left(\xi \wedge \frac{\gamma}{2\sqrt{2d}} \right)$. Finally, for any $t \leq (\varepsilon - \xi)/(32\tau^2\kappa)$ it holds:

$$\mathbb{P} \left(\sup_{x \in \mathbb{R}^d} \left| \hat{D}_{\text{AI-IRW}}(x) - D_{\text{AI-IRW}}(x, P) \right| > t \right) \leq 6.9^d \exp \left(-\frac{n}{2} \min \left\{ (\kappa t)^2, \kappa t \right\} \right) + \frac{6(2n)^{d+1}}{(d+1)!} \exp(-nt^2/32). \quad (13)$$

Bounding each term in the right side by $\delta/2$ and reverting the equation lead to the desired result.

B.2.2. ASSERTION (II)

Let \mathcal{B}_r a centered ball of \mathbb{R}^d with radius $r > 0$ and assume that X satisfies assumption 2 for any $x \in \mathcal{B}_r$. Introducing terms and using triangle inequality, it holds:

$$\begin{aligned} \sup_{x \in \mathcal{B}_r} \left| \tilde{D}_{\text{AI-IRW}}^{\text{MC}}(x) - D_{\text{AI-IRW}}(x, P) \right| &\leq \underbrace{\sup_{x \in \mathbb{R}^d} \left| \hat{D}_{\text{AI-IRW}}(x) - D_{\text{AI-IRW}}(x, P) \right|}_{(1)} \\ &\quad + \underbrace{\sup_{x \in \mathcal{B}_r} \left| D_{\text{AI-IRW}}^{\text{MC}}(x, P) - D_{\text{AI-IRW}}(x, P) \right|}_{(2)} \end{aligned}$$

The first term (1) can be bounded using assertion (i) while controlling the approximation term (2) relies on classical chaining arguments. As the function $z \mapsto \min(z, 1 - z)$ is 1-Lipschitz for any $z \in (0, 1)$ and by triangle inequality, for any y in \mathcal{B}_r we have:

$$\left| D_{\text{AI-IRW}}^{\text{MC}}(y, P) - D_{\text{AI-IRW}}(y, P) \right| \leq \frac{1}{m} \sum_{j=1}^m \left| \mathbb{P} \{ \langle V_j, y \rangle \mid V_j \} - \mathbb{P} \{ \langle V, y \rangle \} \right|.$$

Since it is an average of bounded and i.i.d random variables, combining Hoeffding inequality and union bound, for any $t > 0$ and any y in \mathcal{B}_r it holds:

$$\mathbb{P} \left(\left| D_{\text{AI-IRW}}^{\text{MC}}(y, P) - D_{\text{AI-IRW}}(y, P) \right| > t/2 \right) \leq 2 \exp(-mt^2/2). \quad (14)$$

As X is uniformly continuous Lipschitz in projection for any $u \in \mathbb{S}^{d-1}$, observe that $\forall (x, y) \in \mathcal{B}_r^2$ it holds:

$$\begin{aligned} \left| D_{\text{AI-IRW}}^{\text{MC}}(x, P) - D_{\text{AI-IRW}}(x, P) \right| &\leq \left| D_{\text{AI-IRW}}^{\text{MC}}(x, P) - D_{\text{AI-IRW}}^{\text{MC}}(y, P) \right| + \left| D_{\text{AI-IRW}}^{\text{MC}}(y, P) - D_{\text{AI-IRW}}(y, P) \right| \\ &\quad + \left| D_{\text{AI-IRW}}(x, P) - D_{\text{AI-IRW}}(y, P) \right| \\ &\leq 2L_p \|x - y\| + \left| D_{\text{AI-IRW}}^{\text{MC}}(y, P) - D_{\text{AI-IRW}}(y, P) \right|. \end{aligned} \quad (15)$$

Now let $\zeta > 0$ and $y_1, \dots, y_{\mathcal{N}(\zeta, \mathcal{B}_r, \|\cdot\|_2)}$ be a ζ -coverage of \mathcal{B}_r with respect to $\|\cdot\|_2$. We have:

$$\log(\mathcal{N}(\zeta, \mathcal{B}_r, \|\cdot\|_2)) \leq d \log(3r/\zeta). \quad (16)$$

Set $\mathcal{N} = \mathcal{N}(\zeta, \mathcal{B}_r, \|\cdot\|_2)$ for simplicity. There exists $\ell \leq \mathcal{N}$ such that $\|x - y_\ell\|_2 \leq \zeta$. Thus, Eq. (15) leads to

$$\left| D_{\text{AI-IRW}}^{\text{MC}}(x, P) - D_{\text{AI-IRW}}(x, P) \right| \leq 2L_p \zeta + \left| D_{\text{AI-IRW}}^{\text{MC}}(y_\ell, P) - D_{\text{AI-IRW}}(y_\ell, P) \right|.$$

Applying Eq. (14) to every y_ℓ and the union bound, for any $t > 0$, we get:

$$\mathbb{P} \left(\sup_{\ell \leq \mathcal{N}} \left| D_{\text{AI-IRW}}^{\text{MC}}(y_\ell, P) - D_{\text{AI-IRW}}(y_\ell, P) \right| > t/2 \right) \leq 2\mathcal{N} \exp(-mt^2/2),$$

yielding:

$$\mathbb{P} \left(\sup_{x \in \mathcal{B}_r} \left| D_{\text{AI-IRW}}^{\text{MC}}(x, P) - D_{\text{AI-IRW}}(x, P) \right| > t/2 \right) \leq 2\mathcal{N} \exp(-2m(t/2 - 2L_p\zeta)^2).$$

Using Eq. (13), the union bound and (16), we obtain:

$$\begin{aligned} \mathbb{P} \left(\sup_{x \in \mathcal{B}_r} \left| \tilde{D}_{\text{AI-IRW}}^{\text{MC}}(x) - D_{\text{AI-IRW}}(x, P) \right| > t \right) &\leq \mathbb{P} \left(\sup_{x \in \mathcal{B}_r} \left| \hat{D}_{\text{AI-IRW}}(x) - D_{\text{AI-IRW}}(x, P) \right| > t/2 \right) \\ &\quad + \mathbb{P} \left(\sup_{x \in \mathcal{B}_r} \left| D_{\text{AI-IRW}}^{\text{MC}}(x, P) - D_{\text{AI-IRW}}(x, P) \right| > t/2 \right) \\ &\leq 6.9^d \exp \left(-\frac{n}{2} \min \left\{ (\kappa t/2)^2, \kappa t/2 \right\} \right) \\ &\quad + \frac{6(2n)^{d+1}}{(d+1)!} \exp(-nt^2/128) \\ &\quad + 2 \left(\frac{3r}{\zeta} \right)^d \exp \left(-2m(t/2 - 2L_p\zeta)^2 \right). \end{aligned}$$

Choosing $\zeta \sim m^{-1}$, bounding each term on the right-hand side by $\delta/3$ and reverting the previous equation lead to the desired result.

B.3. Geometrical Results on the Lipschitz Constants of Assumptions 4.3 and 4.4

Lemma B.1. *Let $r > 0$ and denote by $V_{d,r}$ the volume of the d -ball $\mathcal{B}(0, r)$. Assume that X takes its values in $\mathcal{B}(0, r)$ and has an M -bounded density w.r.t. the Lebesgue measure λ . The r.v. X is uniformly RADially LIPSCHITZ CONTINUOUS with constant $L_R = MV_{d,r}$.*

Proof. Let $x \in \mathbb{R}^d$. By $\|\cdot\|_g$ it means the geodesic norm on the unit sphere of \mathbb{R}^d . It holds:

$$\begin{aligned} |\phi(u, x) - \phi(v, x)| &\leq \mathbb{P} \{ X \in \mathcal{B}(0, r) : \langle u, X - x \rangle \text{ and } \langle v, X - x \rangle \text{ are of opposite sign} \} \\ &\leq M \lambda \{ z \in \mathcal{B}(-x, r) : \langle u, z \rangle \text{ and } \langle v, z \rangle \text{ are of opposite sign} \} \\ &\stackrel{(i)}{\leq} M V_{d,r} \times \frac{2}{\pi} \arccos(\langle u, v \rangle) \\ &= M V_{d,r} \times \frac{2}{\pi} \|u - v\|_g \\ &\leq M V_{d,r} \|u - v\|, \end{aligned}$$

Where (i) arises from the fact that the volume of $\mathcal{E}_{u,x,y} = \{z \in \mathcal{B}(-x, r) : \langle u, z \rangle \text{ and } \langle v, z \rangle \text{ are of opposite sign}\}$ is the volume of two cones of angle $\|u - v\|_g$, as depicted in Figure 3. \square

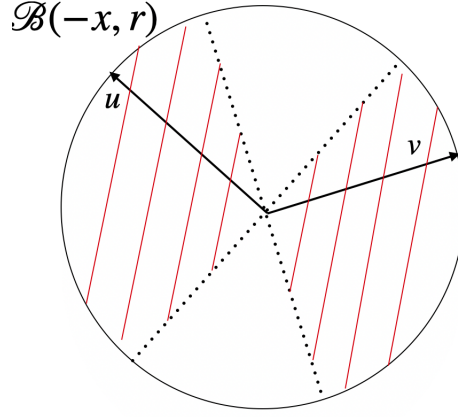


Figure 3. Illustration of the set $\mathcal{E}_{u,x,y}$ in \mathbb{R}^2 . It corresponds to the portion of $\mathcal{B}(-x, r)$ hatched in red.

Lemma B.2. Let $r > 0$ and assume that X takes its values in $\mathcal{B}(0, r)$ and has M -bounded density w.r.t. the Lebesgue measure λ . Thus X is uniformly LIPSCHITZ CONTINUOUS IN PROJECTION with constant $L_p = MV_{d-1,r}$.

Proof. Let $u \in \mathbb{S}^{d-1}$. By $\|\cdot\|_g$ it means the geodesic norm on the unit sphere of \mathbb{R}^d . It holds:

$$\begin{aligned} |\phi(u, x) - \phi(u, y)| &\leq \mathbb{P}\{X \in \mathcal{B}(0, r) : \langle u, X - x \rangle \text{ and } \langle u, X - y \rangle \text{ are of opposite sign}\} \\ &\leq M \lambda\{z \in \mathcal{B}(0, r) : \langle u, z - x \rangle \text{ and } \langle u, z - y \rangle \text{ are of opposite sign}\} \\ &\stackrel{(i)}{\leq} M V_{d-1,r} \times |\langle u, x \rangle - \langle u, y \rangle| \\ &\leq M V_{d-1,r} \|x - y\|. \end{aligned}$$

Where (i) arises from the fact that we encompass $\mathcal{F}_{u,x,y}$ by an hyper-cylinder of length $|\langle u, x \rangle - \langle u, y \rangle|$ where $\mathcal{F}_{u,x,y} = \{z \in \mathcal{B}(0, r) : \langle u, z - x \rangle \text{ and } \langle u, z - y \rangle \text{ are of opposite sign}\}$, as illustrated in Figure 4. \square

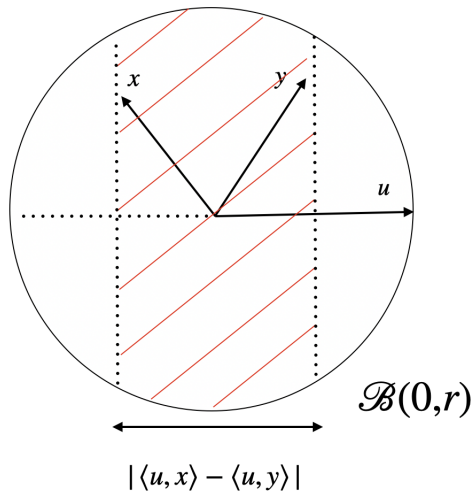


Figure 4. Illustration of the set $\mathcal{F}_{u,x,y}$ in \mathbb{R}^2 . It corresponds to the portion of $\mathcal{B}(0, r)$ hatched in red.

B.4. Finite-Sample Analysis of the IRW depth

A finite sample analysis on IRW can be derived from our results on AI-IRW as it is described in the next corollary.

Corollary B.3. *Suppose that the distribution P of the r.v. X satisfies Assumptions 4.3 and 4.4. Then, for any $\delta \in (0, 1)$, it holds:*

$$\sup_{x \in \mathcal{B}_r} \left| \widehat{D}_{\text{IRW}}^{\text{MC}}(x) - D_{\text{IRW}}(x, P) \right| \leq \sqrt{\frac{8 \log(\Theta/\delta)}{n}} + 2\sqrt{\frac{d \log(3rm) + \log(6/\delta)}{8m}} + \frac{2L_p}{m},$$

where $\Theta = 12(2n)^{d+1}/(d+1)!$.

Proof. First notice that:

$$\sup_{x \in \mathcal{B}_r} \left| \widehat{D}_{\text{IRW}}^{\text{MC}}(x) - D_{\text{IRW}}(x, P) \right| \leq \underbrace{\sup_{x \in \mathbb{R}^d} \left| \widehat{D}_{\text{IRW}}(x) - D_{\text{IRW}}(x, P) \right|}_{(1)} + \underbrace{\sup_{x \in \mathcal{B}_r} \left| D_{\text{IRW}}^{\text{MC}}(x, P) - D_{\text{IRW}}(x, P) \right|}_{(2)}.$$

Now, the first term (1) can be controlled using the bound for the deviations of Halfspace Depth deferred in Lemma A.4. Thus, for any $t > 0$, it holds:

$$\mathbb{P} \left(\sup_{x \in \mathbb{R}^d} \left| \widehat{D}_{\text{IRW}}(x) - D_{\text{IRW}}(x, P) \right| > t/2 \right) \leq \frac{6(2n)^{d+1}}{(d+1)!} \exp(-nt^2/32). \quad (17)$$

The second term can be bounded following the same reasoning than for the Monte-Carlo approximated term of AI-IRW described in Section B.2.2. Thus, with the same notations, for any $t > 0$, we have:

$$\mathbb{P} \left(\sup_{x \in \mathcal{B}_r} \left| D_{\text{IRW}}^{\text{MC}}(x, P) - D_{\text{IRW}}(x, P) \right| > t/2 \right) \leq 2\mathcal{N} \exp \left(-2m(t/2 - 2L_p\zeta)^2 \right). \quad (18)$$

Using Equation (17) and Equation (18), one gets:

$$\begin{aligned} \mathbb{P} \left(\sup_{x \in \mathcal{B}_r} \left| \widehat{D}_{\text{IRW}}^{\text{MC}}(x) - D_{\text{IRW}}(x, P) \right| > t \right) &\leq \mathbb{P} \left(\sup_{x \in \mathcal{B}_r} \left| \widehat{D}_{\text{IRW}}(x) - D_{\text{IRW}}(x, P) \right| > t/2 \right) \\ &\quad + \mathbb{P} \left(\sup_{x \in \mathcal{B}_r} \left| D_{\text{IRW}}^{\text{MC}}(x, P) - D_{\text{IRW}}(x, P) \right| > t/2 \right) \\ &\leq \frac{6(2n)^{d+1}}{(d+1)!} \exp(-nt^2/32) + 2 \left(\frac{3r}{\zeta} \right)^d \exp \left(-2m(t/2 - 2L_p\zeta)^2 \right). \end{aligned}$$

Choosing $\zeta \sim m^{-1}$, bounding each term on the right-hand side by $\delta/2$ and reverting the previous equation lead to the desired result. \square

C. The Approximation Algorithm

In this section, we display the approximation algorithm of the AI-IRW depth, see Algorithm 1.

Algorithm 1 Approximation of the AI-IRW depth

Initialization: The number of projections m .

- 1: Construct $\mathbf{U} \in \mathbb{R}^{d \times m}$ by sampling uniformly m vectors U_1, \dots, U_m in \mathbb{S}^{d-1}
 - 2: Compute $\hat{\Sigma}$ using any estimator
 - 3: Perform Cholesky or SVD on $\hat{\Sigma}$ to obtain $\hat{\Sigma}^{-1/2}$
 - 4: Compute $\mathbf{V} = \hat{\Sigma}^{-1/2} \mathbf{U} / \|\hat{\Sigma}^{-1/2} \mathbf{U}\|$
 - 5: Compute $\mathbf{M} = \mathbf{XV}$
 - 6: Compute the rank value $\sigma(i, j)$, the rank of index i in $\mathbf{M}_{:,j}$ for every $i \leq n$ and $j \leq m$
 - 7: Set $D_i = \frac{1}{m} \sum_{j=1}^m \sigma(i, j)$ for every $i \leq n$
- Output:** D

D. Additional Experiments

D.1. Illustration of (non) Affine-Invariance

The Figure 5 illustrates the non affine-invariance of the IRW and the affine-invariance of the AI-IRW. Indeed, the IRW contours are spherical while the AI-IRW contours are ellipsoidal like those of the underlying Student-10 density.

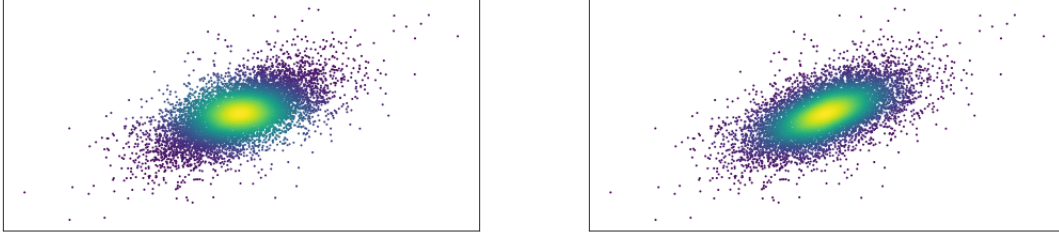


Figure 5. The IRW depth (left) and the AI-IRW (right) depth on a Student-10 distribution. The darker the point, the lower the depth.

D.2. Computation time of the AI-IRW depth using both SC and MCD estimators

Results related to the figure 2 for the IRW depth are depicted in Figure 6. Kendall correlations are close to those of AI-IRW with a slight advantage to the IRW depth as expected due to the presence of an additional covariance estimate term. In addition, computation times related to the first experiment of Section 5 are displayed in Figure 7 for the AI-IRW depth using both SC and MCD estimators as well as the IRW depth.

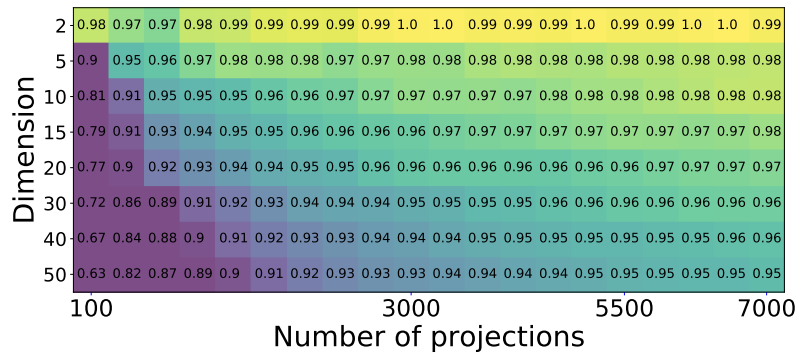


Figure 6. Kendall correlation between the approximated ranks of IRW and its true ranks depending on the number of approximating projections m for a Gaussian distribution.

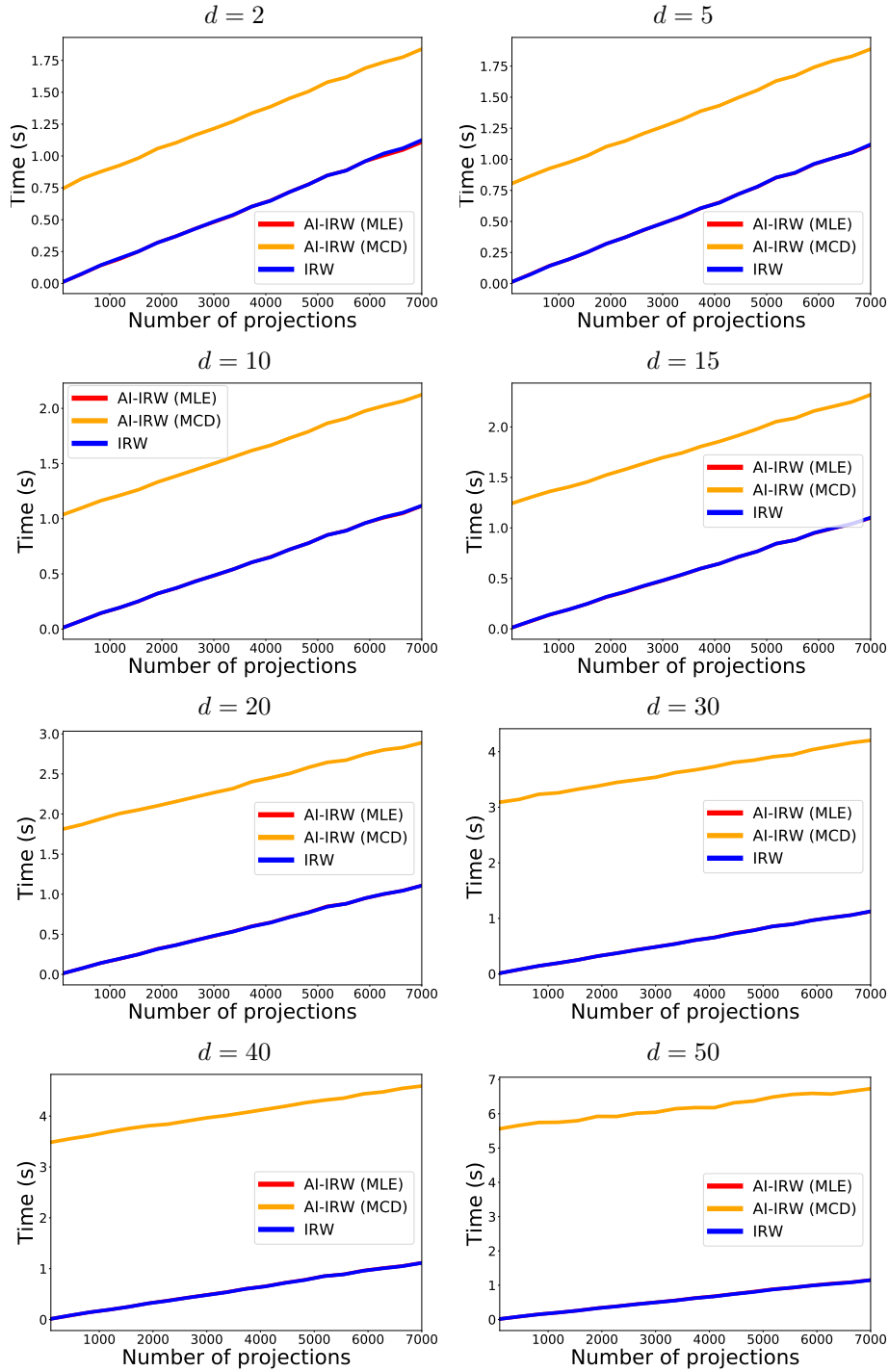


Figure 7. Computation time of the AI-IRW depth using both SC and MCD estimators and the IRW depth depending on the number of projections for various dimensions. AI-IRW and IRW have the same computation time since the computation of the sample covariance matrix is negligible w.r.t. the computation of the IRW depth.

D.3. Anomaly Detection

D.3.1. ANOMALY DETECTION: A COMPARISON ON A TOY DATA SET

In this part, a comparison between AI-IRW, IRW and the halfspace depth is provided. To conduct this experiment, we construct a toy contaminated data set (see Figure 8, left) where aggregated outliers (green points) and some independent outliers (red points) are added to 1000 points stemming from a 2-dimensional *Gaussian* distribution. The 100 lowest scores are depicted (see Figure 8, right) for the three benchmarked data depths. Results show that AI-IRW is able to assign the lowest depth to these anomalies while IRW and Tukey both fail to identify them.

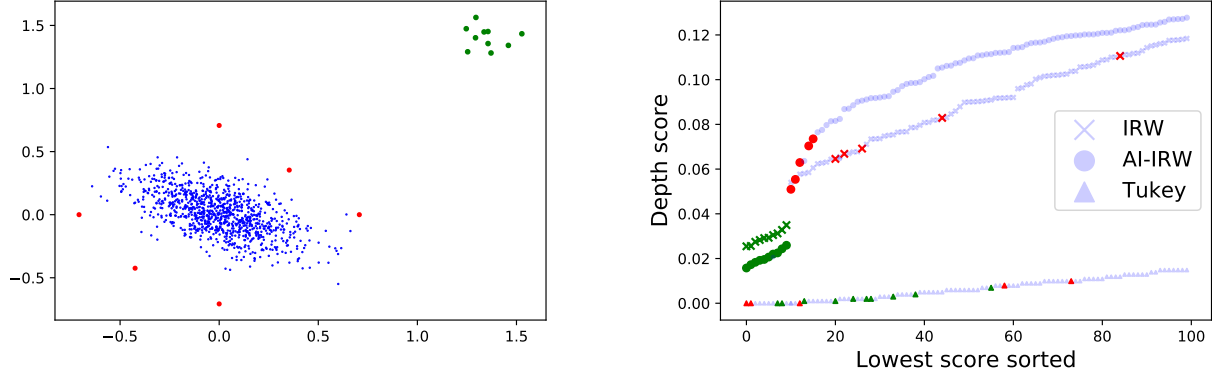


Figure 8. Toy data set with outliers (left) and the AI-IRW, IRW and Tukey sorted scores (right).

D.3.2. COMPUTATION TIME OF BENCHMARKED ANOMALY DETECTION METHODS

Here we provide additional information of the benchmarked data sets used in Section 5 as well as the computation time used to perform the anomaly detection benchmark. Results are displayed in Table 2. AI-IRW, IRW, HM and Tukey are implemented from scratch in python using `numpy` python library. Isolation Forest implementation comes from `scikit-learn` python library (Pedregosa et al., 2011) while the AutoEncoder implementation comes from `pyod` python library (Zhao et al., 2019). All the computations are done on a computer with 3.2 GHz Intel processor with 32 GB of RAM.

	n	d	% of anomaly	$\hat{\gamma} (\times 0.01)$	$\hat{\varepsilon} (\times 0.01)$		
Ecoli	195	5	26	0.3	0.2	AI-IRW	0.04
Shuttle	49097	9	7	9	5.7	IRW	0.005
Mulcross	262144	4	10	100	10^{-10}	HM	0.02
Thyroid	3772	6	2.5	0.01	0.1	T	0.005
Wine	129	13	7.7	0.9	0.9	IF	0.13
Http	567479	3	0.4	19	2.9	AE	9
Smtip	95156	3	0.03	3.9	36		
Breastw	683	9	35	80	20		
Musk	3062	166	3.2	9.4	6		
Satimage	5803	36	1.2	283	2.6		

Table 2. Left: Data sets considered for the performance comparison: n is the number of instances, d is the number of attributes, $\hat{\gamma}$ and $\hat{\varepsilon}$ are the eigengap and the smallest eigenvalue of the SC estimator respectively (left). Right: Computation time of benchmarked anomaly detection methods in seconds.

D.4. Exploring AI-IRW with the MCD Estimator

In this section, we investigate the quality of the approximation as well as the robustness of the AI-IRW depth using both SC and MCD estimators with two experiments.

D.4.1. APPROXIMATION AND ROBUSTNESS

The first experiment is conducted as follows. The accuracy of Monte Carlo approximation, depending on the number m of random directions uniformly sampled, is evaluated for the empirical versions of the AI-IRW depth using SC and MCD estimators as well as the IRW depth. The experiment is based on samples of size $n = 1000$ drawn from the multivariate standard Gaussian distribution (standard, so that non affine invariant depth are not disadvantaged) in dimension $d = 5$. The classical Kendall τ distance, given by

$$d_{\tau}(\sigma, \sigma') = \frac{2}{n(n-1)} \sum_{i < j} \mathbb{I}_{\{(\sigma(i) - \sigma(j))(\sigma'(i) - \sigma'(j)) < 0\}},$$

for all permutations σ and σ' of the index set $\{1, \dots, n\}$, is used to measure the deviation between the ranks induced by the “true” depth (approximated with $m = 200000$ projections since there exists no closed-form) and those defined by the Monte Carlo approximation of the sampling version. The averaged Kendall τ ’s (over 10 runs), that correspond to one minus the Kendall correlations, are displayed in Figure 9. One observes that the approximate empirical AI-IRW depth is not affected by the covariance estimation step, its behavior is similar to that of the approximate empirical IRW depth for the Gaussian distribution when using both covariance estimators. On the other hand, a slight advantage is awarded to MCD under the heavy-tailed Student-3 model.

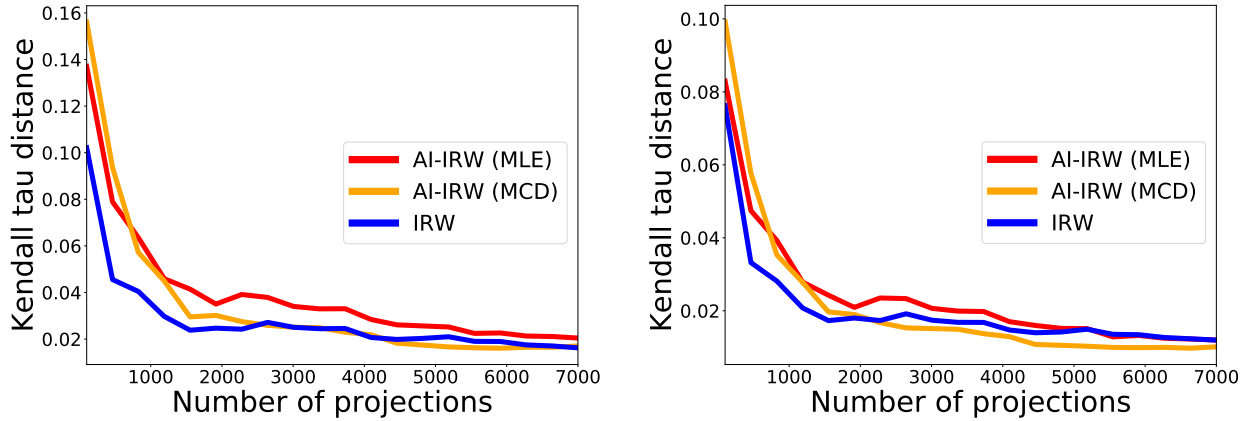


Figure 9. Coherence of the returned rank measured by Kendall τ distance depending on the number of approximating projections for Gaussian (left) and Student-3 (right) distributions for AI-IRW (using SC and MCD estimates) and IRW.

D.4.2. ROBUSTNESS W.R.T. INCREASING PROPORTION OF OUTLIERS

In the second experiment, we examine the robustness of the returned ordering. It is based on the construction of two contaminated data sets from samples of size $n = 100$ drawn from the multivariate standard Gaussian distribution (standard, so that non affine invariant depths are not disadvantaged) in dimension $d = 2$. To build corrupted data set, the two following contaminated models are used. The first is based on adding “isolated outliers” where each of them is defined as $(0, a)$ where a is sampled uniformly between $[4, 400]$. The second is based on adding “aggregated outliers” by randomly and uniformly drawing a location b in $[4, 400]$ and then drawing anomalies following the Gaussian distribution $\mathcal{N}(\mathbf{b}, \mathcal{I}_2)$ where \mathbf{b} is the vector (b, b) . Therefore, each data set is constructed as follows: a proportion of outliers $\alpha \in [0, 0.15]$ is added to the normal data, represented by the standard Gaussian distribution, following one of the two aforementioned contamination models and thus yields two settings. The AI-IRW depth using SC and MCD estimators as well as the IRW depth are computed on these contaminated data sets. The Kendall τ distance is used to measure the deviation between the “true” ranks that are computed on samples without corruption and those computed on samples with corruption w.r.t. a proportion of anomalies α . The averaged Kendall τ ’s (over 100 runs) are displayed in Figure 10. As expected, results show that the MCD estimator provides robustness to the AI-IRW depth while the sample covariance estimator breaks down after only 1% of anomalies. Interestingly, the MCD estimator does not bring more robustness than the underlying robustness of the IRW depth. It highlights somehow a “worst case” robustness between the estimator of the covariance matrix and the underlying IRW depth which is reached by the latter.

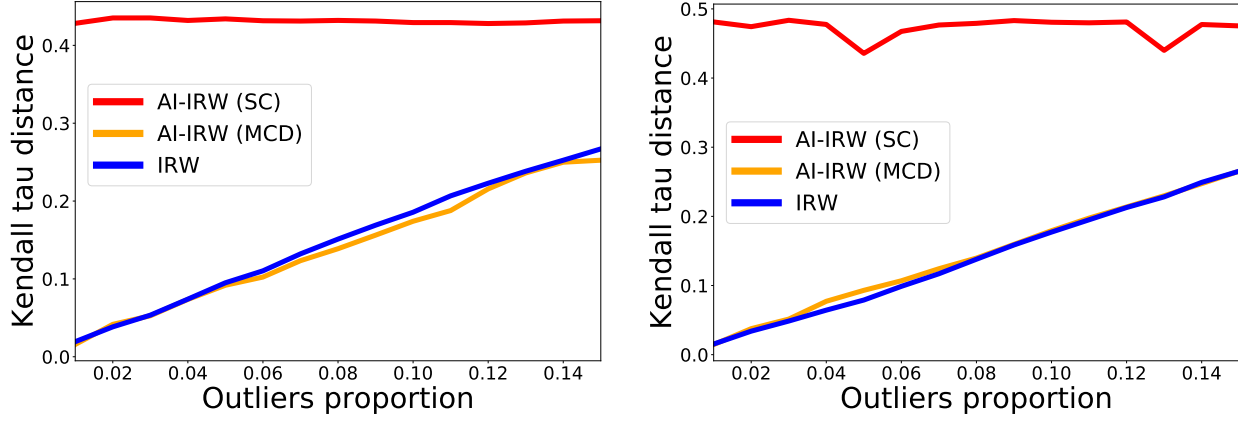


Figure 10. Coherence of the returned rank measured by Kendall τ depending on outliers proportion for Student-3 (left) and Gaussian (right) distributions for AI-IRW (using SC and MCD estimates) and IRW.

D.5. Variance of AI-IRW Score

D.5.1. VARIANCE W.R.T. SAMPLE REALIZATIONS

We compare the stability of the approximation estimator AI-IRW measuring its variance. For 100 points stemming from a 10-dimensional Gaussian distribution with zero mean and covariance matrix drawn from the Wishart distribution (with parameters (d, \mathcal{I}_d)) on the space of definite matrices, the variance of the returned score is computed on two points, denoted by x_1 and x_2 , drawn randomly from the 100 points previous points. The score is computed for AI-IRW, IRW, halfspace mass and halfspace depths each approximated using $m = 100$ directions. Figure 11 illustrates that (1) no additional variance is introduced by the affine-invariant version, (2) closeness of the three scores (due to absence of correlation), as well as (3) their higher concentrations compared to halfspace mass and halfspace depth.

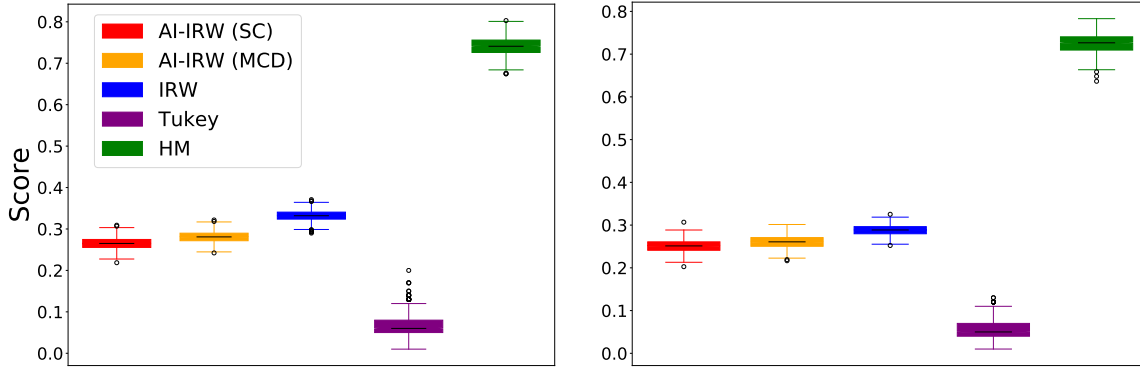


Figure 11. Variance of the score of x_1, x_2 (from left to right) over 1000 repetitions for the AI-IRW, IRW, halfspace mass (HM) and halfspace (Tukey) depths.

D.5.2. VARIANCE W.R.T. NOISY DIRECTIONS

The experiment in Section D.5.1 is repeated with different level of Gaussian noise that are added to sampled directions, i.e. $U = \frac{W + \varepsilon \mathcal{N}(\mathbf{0}, \mathcal{I}_d)}{\|W + \varepsilon \mathcal{N}(\mathbf{0}, \mathcal{I}_d)\|}$. This experiment is conducted with AI-IRW, IRW, HM and halfspace depth using $m = 100$ sampled directions. The root mean square variance (over 100 repetitions) between the returned score and the original score (without noise) are computed for x_1, x_2 (same as those in Section D.5.1), see Figure 12. Results show that AI-IRW (using the SC estimator) shares very few differences with IRW while the superiority of AI-IRW (and IRW) over the existing methods depth such as halfspace and halfspace mass is highlighted.

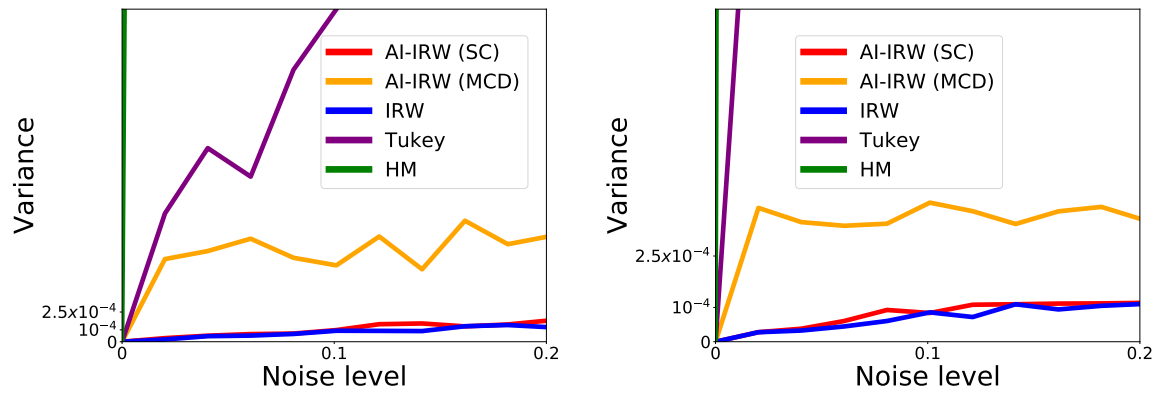


Figure 12. Variance of the score of x_1, x_2 (from left to right) over the noise level induced in sampled directions with 1000 repetitions for the AI-IRW, IRW, Tukey depth.